



저작자표시-비영리-변경금지 2.0 대한민국

이용자는 아래의 조건을 따르는 경우에 한하여 자유롭게

- 이 저작물을 복제, 배포, 전송, 전시, 공연 및 방송할 수 있습니다.

다음과 같은 조건을 따라야 합니다:



저작자표시. 귀하는 원저작자를 표시하여야 합니다.



비영리. 귀하는 이 저작물을 영리 목적으로 이용할 수 없습니다.



변경금지. 귀하는 이 저작물을 개작, 변형 또는 가공할 수 없습니다.

- 귀하는, 이 저작물의 재이용이나 배포의 경우, 이 저작물에 적용된 이용허락조건을 명확하게 나타내어야 합니다.
- 저작권자로부터 별도의 허가를 받으면 이러한 조건들은 적용되지 않습니다.

저작권법에 따른 이용자의 권리는 위의 내용에 의하여 영향을 받지 않습니다.

이것은 [이용허락규약\(Legal Code\)](#)을 이해하기 쉽게 요약한 것입니다.

[Disclaimer](#)

工學碩士 學位論文

Changes of the Structural and Mechanical Properties on
Nanocomposites based on Halloysite Nanotubes with the
Optimization of Dispersion by Ultrasonic Waves

초음파에 의해 최적 분산된 할로이사이트 강화 나노 복합재료의 구조적 및 기계적
물성 변화에 관한 연구



指導教授 金 允 海

2016年 2月

韓國海洋大學校 大學院
造船機資材 工 學 科

朴 水 庭

本 論 文 을 朴 水 庭 의 工 學 碩 士 學 位 論 文 으 로
認 准 함.



2015년 12월 23일

韓 國 海 洋 大 學 校 大 學 院

Contents

| | |
|-----------------------|----|
| List of Tables | iv |
| List of Figures | v |
| Abstract | vi |

1. Introduction

| | |
|---|----|
| 1.1 Nanocomposites | 1 |
| 1.2 Halloysite Nanotube (HNT) as an Eco-friendly Material | 8 |
| 1.3 Effective Dispersion of Nanofillers in Nanocomposites | 11 |

2. Experimental Work

| | |
|--|----|
| 2.1 Materials and Methods | 15 |
| 2.1.1 Preparation of UP/HNT Nanocomposites | 15 |
| 2.1.2 Heat Treatment of HNTs at Different Temperatures | 22 |
| 2.1.3 HNT Dispersion by Ultrasonic Homogenization | 25 |
| 2.2 Characterization of UP/HNT Nanocomposites | 28 |
| 2.2.1 X-ray Diffraction | 28 |
| 2.2.2 Transmission Electron Microscopy (TEM) | 30 |
| 2.2.3 Impact Test | 31 |
| 2.2.4 Tensile Test | 33 |

| | |
|---|----|
| 3. Results and Discussion | |
| 3.1 Observation of Structural Changes by X-ray Diffraction and TEM Imaging | 36 |
| 3.2 Changes in Mechanical Properties | 44 |
| 3.2.1 Impact Properties | 44 |
| 3.2.2 Tensile Properties | 49 |
| 3.2.3 Considerations on the Effects of Nanoparticle Dispersion on Mechanical Strength | 54 |
| | |
| 4. Conclusion | 57 |
| | |
| Reference | 59 |
| | |
| Acknowledgment | 64 |



List of Tables

| | |
|---|----|
| Table 2.1 Description of main materials | 16 |
| Table 2.2 Conditions of ultrasonic homogenization used | 26 |



List of Figures

| | |
|--|----|
| Fig. 1.1 Curing reaction of thermoplastic resin | 4 |
| Fig. 1.2 Structure of thermosetting resin | 5 |
| Fig. 1.3 Classification of composite material according to the component | 7 |
| Fig. 1.4 Comparison of nanofiller dispersion method as observed by optical microscope | 13 |
| Fig. 2.1 Manufacture of polyester resins based on coal and petroleum | 17 |
| Fig. 2.2 Matrix and addition | 18 |
| Fig. 2.3 HNTs at room temperature | 19 |
| Fig. 2.4 Chemical structure of HNT | 19 |
| Fig. 2.5 Sample preparation procedure | 20 |
| Fig. 2.6 Schematic diagram of resin infusion and shape preservation | 22 |
| Fig. 2.7 Heat treatment machine | 23 |
| Fig. 2.8 Process diagram of heat treatment | 24 |
| Fig. 2.9 Ultrasonic homogenization machine | 25 |
| Fig. 2.10 Process schematic diagram of ultrasonic homogenization | 28 |
| Fig. 2.11 Equipment used for impact test and the samples | 32 |
| Fig. 2.12 Machine for tensile test | 33 |
| Fig. 2.13 Samples for tensile test | 34 |
| Fig. 3.1 X-Ray observation of HNTs at various heat treatment temperatures ... | 38 |
| Fig. 3.2 TEM of HNTs at various temperatures | 41 |
| Fig. 3.3 Comparison of impact strength of neat UP and its nanocomposites under 45W of ultrasonic homogenization condition | 46 |
| Fig. 3.4 Comparison of impact strength of neat UP and its nanocomposites under 60W of ultrasonic homogenization condition | 47 |
| Fig. 3.5 Results of tensile test of neat UP and its nanocomposites under 45W of ultrasonic homogenization condition | 51 |
| Fig. 3.6 Results of tensile test of neat UP and its nanocomposites under 60W of ultrasonic homogenization condition | 53 |

초음파에 의해 최적 분산된 할로이사이트 강화 나노 복합재료의 구조적 및 기계적 물성 변화에 관한 연구

Park, Soo Jeong

Department of Marine Equipment Engineering
Graduate School of Korea Maritime and Ocean University

Abstract

Nanoparticle refers to a particle within the scope of a hundred nanometers and nanoparticles have a wide specific surface area. By controlling their size or using nanoparticles of various types, the properties of material can be improved with only a small amount of particulate filler.

Halloysite is a naturally occurring aluminosilicate in the form of nanotubes, also known as halloysite nanotubes (HNTs). The HNTs are odorless, white particles with the chemical formula $H_4Al_2O_9Si_2 \cdot 2H_2O$. Halloysite nanotubes are readily obtainable and are much cheaper than other tubular nanoparticles such as carbon nanotubes. There HNTs have been considered as a functionally effective material capable of mechanically strengthening resins by restrictive matrix dislocation movement. Especially, there are studies showing that adding HNTs to plastics improves tensile strength, impact resistance, fire retardancy and gives the added advantage of improved cycling time in production by injection molding.

In this study, samples consisted of nanocomposites manufactured by adding HNTs to unsaturated polyester resin (UP). Herein, the contents of HNTs were 0.5, 1 and 3 wt.%. The purpose was to analyze the mechanical properties of nanocomposites on a function of HNTs content and through this, to find the optimal conditions for developing UP matrix HNT reinforced nanocomposites. The HNTs used in this study were treated by heat. Heat-treated HNTs were divided into 4 groups: untreated HNT (UTHNT), 300°C (300HTHNT), 500°C (500HTHNT), 700°C (700HTHNT) and 1000°C (1000HTHNT) heat-treated HNT, according to treating temperatures. To achieve a uniform distribution of nanoparticles in the matrix, the factors optimized for dispersion were considered and a suitable process environment for materials to be used was adopted by dividing these factors into constants and variables. The ultrasonic homogenization is used in the production of nano-size materials, dispersions and emulsions, because of the potential in deagglomeration. Ultrasonic homogenization is an easy way to separate particle aggregate, and obtain homogeneous phase. Ultrasonication was carried out by varying some parameters. The operating time and the volume of the sample were maintained at fixed values, namely 300 s and 18 ml, respectively. The output power was divided into two cases, at 45W and 60W.

Finally we established the optimal dispersion condition of HNTs using ultrasonication, and the reinforcement effect of HNTs was studied by X-ray diffraction and evaluation of mechanical properties of nanocomposites such as impact strength and tensile strength. Also, the structural changes of HNT by heat treatment at various temperatures were evaluated.

KEY WORDS: Unsaturated polyester resin 불포화 폴리에스테르 수지; Halloysite Nanotube 할로이사이트 나노튜브; Nanocomposites 나노복합재료; Ultrasonic homogenization 초음파 분산, Mechanical property 기계적 특성

Chapter 1 Introduction

1.1 Nanocomposites

Nanoparticles refer to particles whose diameter ranges typically from a few to hundreds of nanometers. Nanotechnology is currently a core technology employed in almost all high-tech industries around the globe. And Nanotechnology primarily involves producing suitable smart materials either by controlling the size of the nanoparticles or by using nanoparticles of various types. When nanoparticles are added to composite materials, such as in polymer matrix composites (PMC), the mechanical properties of the material are improved and composites with added nanoparticles behave as multi-functional materials. For example, toughness and modulus of elasticity of resin are increased by compounding filler in particulate form to the resin (Park, J.H & Kim, J.Y., 2002). Since nanoparticles have a large surface area, improved electrical, mechanical and thermal properties can be achieved with only a small amount of the particulate filler.

However, these particulate fillers also introduce certain defects within the resin. This is because the particulate filler can act as sources of stress concentration. Prior research found that the mechanical strength of resin depends on the amount of particulate filler added to the resin. It was found that addition of particulate fillers of diameter less than 10 μm could reduce defects in the resin (Moloney, et al., 1987 cited in Park & Kim, 2002). Such high-strength plastic reinforced by nanoparticles is an example of nanocomposite.

Generally, a composite material which typically comprises two or more

different materials displays enhanced properties with respect to density, rigidity and impact resistance. Composite materials mainly originated from the need for new materials for different requirements. Depending on the properties and advantages of usage, composite materials have diverse applications. For example, composite materials used in harsh environments, such as in the sea can be easily molded and used where sudden temperature changes occur or in high salt concentration. Therefore, the composite materials can improve the characteristic such as strength, stiffness, corrosion resistance, fatigue life, wear resistance, impact properties, weight ratio and thermal stability (Abdullayev, E. & Lvov, Y., 2010). Composite materials are used in many applications, such as the body and wings of airplanes; lamp housings and bumpers of cars; hull, deck and mast of boats; and pipes, storage tanks, pressure vessels, furnishings, electronics, sporting goods, etc.

Composite materials generally consist of a matrix and reinforcement materials (say, nanoparticles), which increase the strength and rigidity of the matrix. There are 3 kinds of the composite materials depending on the matrix type, i.e. Ceramic Matrix Composites (CMC' s), PMC' s and Metal Matrix Composites (MMC' s). First, CMC' s are composed of a ceramic-based matrix reinforced by short fibers of silicon carbide or boron nitride. The ceramic matrices are oxides, nitrides and carbides of different metal elements, e.g. aluminum, silicon, titanium, and zinc. The ceramic has a strong inter-atomic coherence, high hardness, chemical stability, low toughness, high brittleness and low impact resistance, and plays important role as an insulator of electricity and heat. Thus, CMC' s can be used in high temperature applications. Second, PMC' s are the most common composite comprising polymers, plastics, resins and various fiber reinforcements, such as glass, carbon, and aramid fibers.

Third, in MMC's the matrix is metal based, e.g. aluminum, and fibers, such as silicon carbide.

In general, polymers have a number of limitations for using in structural materials because the mechanical properties of the polymer are not as strong as those of the metals. However, the polymers distribute the load applied to a composite material to individual fibers, while preventing damage of the fibers from abrasion and impact. Thus, when the polymer is used as composite materials rather than as a single material like metals, it is possible to obtain superior properties from the polymer than metals. In addition, main properties like high strength and rigidity, easy formability of complex shapes and excellent environmental resistance, tend to show up compared to metals, with added benefit of lower density relevant in a number of application areas. Therefore, PMC's offer unique properties and have received much attention as a potential composite material.

All resin used in composite materials requires the following characteristics: excellent mechanical properties, adhesion performance, toughness, resistance against environmental degradation. A number of resins are currently used in industry and each of these has different properties. However, they all show a common characteristic which is that the resins are composed of long-chain of macromolecules made up of a number of molecules in simple recurring units. These resins are typically classified as thermoplastic resins (Fig. 1.1) and thermosetting resins (Fig. 1.2) which behave differently under the influence of heat. The thermoplastic resin has a reversible reaction to heat, showing a reversible physical change (solid to liquid) under heat, i.e. it is liquefied by heating and solidified by cooling. The crossing of a softening point or

melting point is repeatable regardless of the physical properties of the material in the respective states. Also, the chemical structure of thermoplastics remains unchanged during heating and forming.

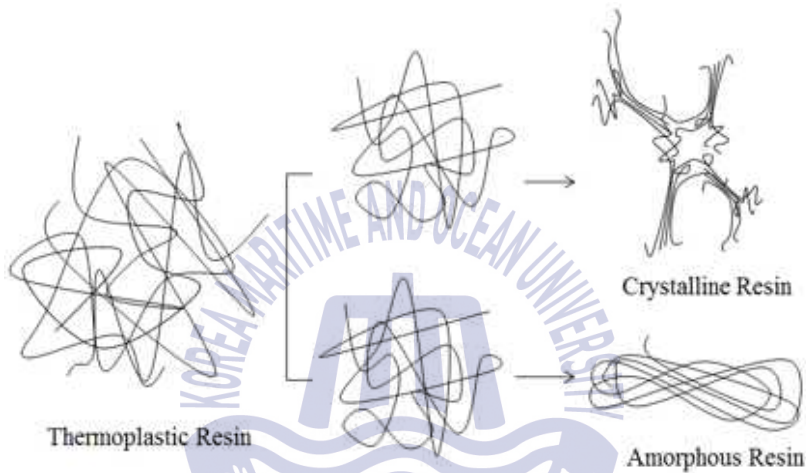


Fig. 1.1 Curing reaction of thermoplastic resin

On the other hand, a thermosetting resin is formed by chemical reaction. The resin and hardener or the resin and accelerator is cured by an irreversible chemical reaction. In some thermosetting resins, such as phenolic resin, volatile by-products are formed through condensation reaction. However, processing of other thermosetting resins, such as polyester or epoxy is easy since they do not generate volatile by-products when cured. Unlike thermoplastic resins, when a

thermosetting resin is cured, it is not liquefied by heat even if the temperature that would greatly change its mechanical properties is attained. In other words, a thermosetting resin cannot be re-melted. Undergoing the curing process through heating and shaping causes a permanent change (called cross-linking) in the molecular structure and the temperature at a cross-linking time is referred to as the glass transition temperature (T_g). The T_g changes depending on the type of resin, the curing process and the mixing ratio with hardener and accelerator. At temperatures above T_g , the thermosetting resin converts to flexible and amorphous polymers from rigid molecular structure of the polymer crystals. This change is reversible below T_g (Albdiry, M.T. Ku, H. & Yousif, B.F., 2013).



Fig 1.2 Structure of thermosetting resin

Depending on the type of reinforcement, a composite material can be classified into three types- fiber, particle and flake reinforcement. Generally reinforcement has a major role in the strength and a rigidity of material. The choice of reinforcements depends on many factors,

such as specific gravity, tensile strength and tensile stiffness, compressive strength and compressive stiffness, fatigue strength and fatigue failure mechanism, electrical and thermal conductivities and price. To determine the physical properties of the reinforcements, generally the type, amount and lamination angles of the reinforcement are taken into account, and using this information, relationship between the matrix and the reinforcement materials can be deduced. For example, reinforcement fibers can greatly restrict formation of any crack when used in a matrix having high brittleness (Na, H.Y. Yeom, H.Y. Yoon, B.C. & Lee, S.J., 2014). By contrast, for particles, the composite materials are prone to develop cracks easily. Additionally, the particles receive considerable mechanical stress, and thus are considered as a weak reinforcing material.

That is, the particles act as foci of stress concentration. However, the particles can help suppress plastic deformation of the matrix effectively even under high load. The third reinforcement material, i.e., the flake has a more flattened shape than the particles and has similar characteristics as that of the particles. In addition, reinforcements are classified as fiber-reinforced, flake-reinforced, particulate-reinforced and skeletal-reinforced according to the shape of the particles and there are also various types depending on the strengthening types of reinforcement. Fig. 1.3 shows a diagram of different components of composite materials.

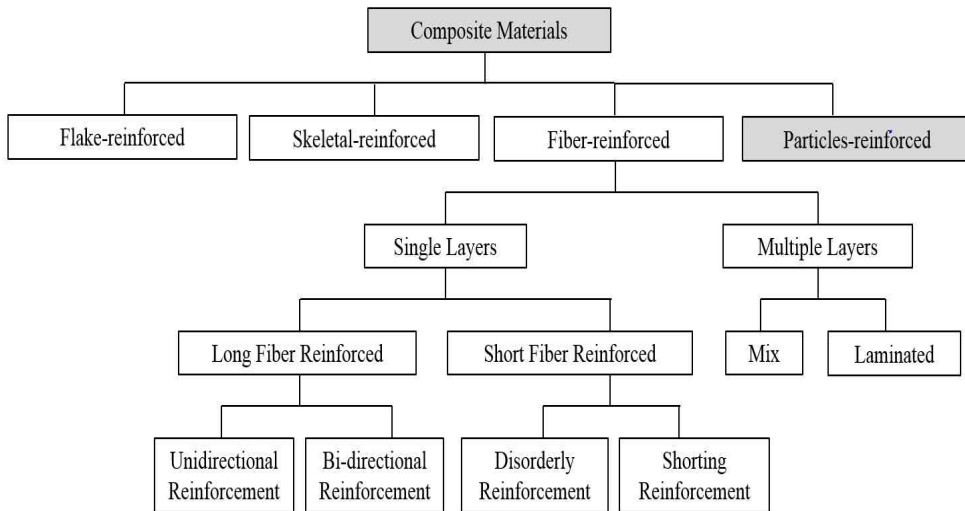


Fig. 1.3 Classification of composite material according to the component

Especially in particle reinforced composites, geometric and spatial characteristics of the dispersed particles affect the properties of the composite material, and thus, needs special attention. The primary characteristics of the particles that affect the properties of the composite materials are concentration, size, shape, distribution and orientation of the dispersed phase.

For strengthening the polymer by particles, the pores are trapped inside the matrix/particle colloidal solution which deteriorates the properties of the composite materials. Water can easily enter through these pores which also can act as stress concentration. It is difficult to determine the precise mechanical properties from the dispersing strength and stiffness data as well as reducing resistant of fatigue. Therefore, fabrication of such composite materials should target minimal

incorporation of pores within the matrix to achieve maximum particle reinforcement effect. An optimum processing methodology needs to be developed depending on the size of the particles used to yield a good composite material.

1.2 Halloysite Nanotube (HNT) as an Eco-friendly Material

The HNTs are eco-friendly nanotubes with lower cost than carbon nanotubes (CNTs). Recently, there has been a growing concern on the effect of CNT on human health and on the environment because of their possible toxic nature (Kamble, R. Ghag, M. Gaikawad, S. & Panda, B.K., 2012). At the same time, HNTs are nowadays under the spotlight. Advanced studies showed that HNT are non-toxic toward living cells (Vergaro, V. et al., 2010 cited in Deen, I. & Zhitomirsky, I., 2014).

The HNTs are important inorganic components of composite nanomaterials in various areas, such as corrosion protection of implanted alloys, controlled delivery of drugs and antimicrobial agents (Deen, I. & Zhitomirsky, I., 2014). HNT is a naturally occurring polymorph of kaolinite, $\text{Al}_2\text{Si}_2\text{O}_5(\text{OH})_4 \cdot 2\text{H}_2\text{O}$, with a dominant hollow tubular morphology (Joussein et al., 2005, 2007 cited in Carli, L.N. et al., 2013). The HNTs are unique and is an all-purpose nanomaterial consisting of a double layer of aluminum, silicon, hydrogen and oxygen. HNTs are formed due to strain developed from lattice mismatch between adjoining silicon dioxide and aluminum oxide layers. The main advantages of the HNTs are that they are natural and non-toxic materials, have acceptable particle size, and high surface area (Kamble, R. Ghag, M. Gaikawad, S. & Panda, B.K., 2012). Furthermore, the HNTs can improve the thermal

and impact characteristics of the composite matrix (Fujii, K. Nakagaito, A.N. Takagi, H. & Yonekura, D., 2014). The addition of nanoparticles reduces specific wear rate (Romanzini, D. Frache, A. Zattera, A.J. & Amico, S.C., 2015).

Structurally, the HNT is made up of kaolinite-like aluminosilicate layers interspersed in the completely hydrated mineral with a sheet of water molecules. The HNT has two different interlayer surfaces. The external surface is principally covered by some silanol (Si-OH) and aluminol (Al-OH) groups and siloxane (Si-O-Si) groups, but remains uncovered at the edges of the tube. The internal surface is covered by aluminol groups (Guo, et al., 2008 cited in Carli, L.N. et al., 2013; Zhang, Y. He, X. Ouyang, J. & Yang, H., 2013). Moreover, HNT, similarly like the other polymorphs of kaolinite, includes 2 types of hydroxyl groups: the outer hydroxyl groups (OuOH) and the inner hydroxyl groups (InOH). The OuOH are located in the outer-upper unshared plane, while the InOH groups are present in the lower shared plane of the octahedral sheet (Frost, R.L. & Shurvell, H.F., 1997). However, the dissimilarity between HNT and kaolinite is that there is a thin layer of water between continuing layers. This layer relaxes the necessity of positional registry between the layers and by doing so, permits for bending. The curvature forms towards the side with the alumina surface (Li, X. et al., 2013).

There are clear advantages in using HNT as filler for reinforced polymer composites. First is the ease of manufacturing specimens, because HNTs are mostly nanotubes with no or little surface charge. Such nanotubes may eliminate the need for intercalation and exfoliation, as required by other two-dimensional nanoclay fillers, such as montmorillonites (MMTs), to blend with polymers and achieve

homogeneous particle dispersion (Deng, S. Zhang, J. & Ye, L., 2009).

Prior reports showed that addition of 3 wt.% HNTs to plastics can improve the tensile strength, impact resistance, fire retardance and give the added benefit of improved cycling time in manufacturing process because HNTs are nucleating agents that form a skeletal framework in polymers. Especially, when considering tensile and inter-laminar shear strengths in glass fiber-reinforced plastics (GFRP)/HNTs nanocomposites containing HNTs over 3 wt.%, the strengths were lower than pure composite, with property improvement limited to a slightly higher extent. Exceptions were nanocomposites reinforced with 0.5 and 1 wt.% HNTs (Kim, Y.H., Park, S.J., Lee, J.W. & Moon, K.M., 2015).

However, HNTs, being inorganic compounds, typically do not have good interaction with organic polymers, resulting in poor dispersion and adhesion (Bellucci, et al., 2007 cited in Carli, L.N., 2013).

Thus, in this study, by combining the HNT as an eco-friendly material with a conventional matrix we attempted to improve the properties of the composite materials. Especially, when unsaturated polyester resin (UP) is cured, it displays a relatively large heat shrinkage and low thermal stability above 80°C, so the improvement in the mechanical properties of UP is required to expand the resin's range of applications (Lee, J.M. & Cho, D.H., 2003). In this regard, the addition of HNTs is a good option to obtain a cost-effective and versatile (multi-utility) nanocomposite.

1.3 Effective Dispersion of Nanofillers in Nanocomposites

For nanofillers used in reinforcement of matrix, the dispersion method is an important factor in realizing improved properties of the composite materials. Recent research shows that the interfacial interactions and degree of dispersion of fillers in the matrix is important in determining the final performance of nanocomposites (Prashantha, K. Lacrampe, M.F. & Krawczak, P., 2013) and that a modification of the conventional production process is required because of changes in rheological properties of the matrix caused by the nanofillers. Therefore, it is also necessary to optimize the dispersion of the nanoparticles in the resin to achieve a homogeneous distribution and also study the influence of nanoparticles on the viscosity of the resin (Park, J.H. & Kim, J.Y., 2002).

Nanocomposites are formed when particles with a diameter of 20–200 *nm* in size are added to the resin. This addition renders new physical properties to the resin. Recently, many studies have been done with silicate clay particles which are 8 to 10 μm in size. The silicate clay has a layered structure having a thickness of 1 *nm* and the individual clay layers can be exfoliated by intercalation or delamination to obtain a higher strength than ordinary solid clay particles (Park, J.H. & Kim, J.Y., 2002).

A typical method of dispersion involves dispersion of nanofiller by additives. When using the additive in a homogeneous dispersion, measurement of the inherent properties of the material is possible. However, the role and influence of additives on dispersion is not completely understood to date (Kim, D.H. Zheng, X.R. Kim, M.S. & Park, C.W., 2012). In addition, dispersion is usually carried out through

mechanical dispersion, ball milling and ultrasonic homogenization. The mechanical dispersion is a passive process and is greatly influenced by the external environment such as the dispersion rate and input power and so it is difficult to obtain a standardized system. There also remains a large characteristic difference between each of the composite materials prepared through mechanical dispersion. By contrast, for ball milling and ultrasonic homogenization, the influence of the external environment is less and the difference in properties between the composite materials prepared under different external conditions is less, but technical limitations still exist for these dispersion methods. The typical usages of ball milling include particle size reduction, solid-state alloying and particle form alteration and moreover, mixing using a ball mill are also an effective process to make a homogeneous mixture of polymer with nanofillers. During ball milling, centrifugal forces of the grinding balls create high shear forces to segregate the fine particles in agglomerates of nanofillers, thereby affecting the mixture in the grinding bowl (Deng, S. Zhang, J. & Ye, L., 2009).

Ultrasound is a representative method for contraction of aggregate particle size in dispersions and emulsions. The dispersing and deagglomeration of solids into liquids are an important application of ultrasonic apparatus. Ultrasound is extensively used in chemical, physical and biological processes. Homogenizing, dispersing and emulsifying are physical processes (Hielscher, T., 2005; Lionetto, F. & Maffezzoli, A., 2013). Ultrasound is also used in laboratory and bench-top scale before the process is scaled up to the commercial stage. High intensity ultrasonication is an alternative to these technologies such as high pressure homogenizers, agitator bead mills, impinging jet mills and rotor-stator-mixers, and particularly for the particle treatment in the

nanosize range, the only effective method to accomplish the required results. Ultrasonic homogenization imparts an immediate effect by applying direct pressure to the nanofillers and is considered as an appropriate dispersion method because the results can be predicted by adjusting the test conditions unlike in the ball milling.

Fig. 1.4 shows optical micrographs of mechanical dispersion and ultrasonic homogenization that directly affect the nanofillers most importantly, ultrasonic homogenization also inhibits aggregation of nanoparticles in the system. However, for mechanical dispersion, the nanoparticles remain in large agglomerated forms and no matrix was found to be combined with the particles. This has a significant effect on the mechanical properties of the material and in such a scenario the nanofillers cannot act as a reinforcement material.

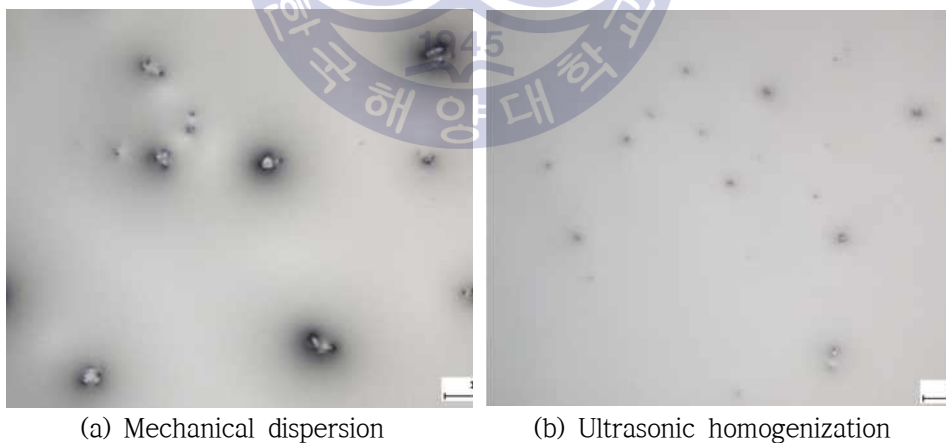


Fig. 1.4 Comparison of nanofiller dispersion method as observed by optical microscope

Therefore, it is important to choose the appropriate dispersion method for matrix and nanofillers to realize a reinforced nanocomposite. Achieving a homogeneous dispersion of nanofillers in the matrix still remains a problem owing to the agglomeration of nanoparticles that form large particle clusters (Deng, S. 0Zhang, J. & Ye, S., 2009 cited in Deng, S. et al., 2008). Thus, in order to establish an optimum dispersion of the HNTs the current study has selected ultrasonic homogenization, where variables are easy to set and intended results can be obtained.



Chapter 2 Experimental Work

2.1 Materials and Methods

2.1.1 Preparation of UP/HNT Nanocomposites

The purpose of this study was to analyze the variation of mechanical properties of nanocomposite with respect to the contents of HNTs and thereby, to find the optimal conditions for the synthesis of HNT reinforced nanocomposite.

The materials used in this study are shown in table 2.1. The nanocomposite specimens were composed of unsaturated polyester resin (UP) as matrix which is a representative thermosetting resin (Osman, E.A. Vakhguelt, A. Sbarski, I. & Mutasher, S.A., 2012) and HNTs reinforcement. The HNT, a naturally occurring aluminosilicate nanotube, is an odorless, white particle with chemical formula of $H_4Al_2O_9Si_2 \cdot 2H_2O$. The samples of HNTs particle-reinforced UP matrix nanocomposites manufactured were distinguished based on contents of HNTs added to UP.

Table 2.1 Description of main materials

| Materials | Provider | Specifications |
|-------------------------------------|---|--|
| Reinforcement | Sigma-Aldrich | • Formula : $H_4Al_2O_9Si_2 \cdot 2H_2O$ |
| Halloysite | Japan G.K. | |
| Nanotube (HNT) | Product No. 685445 CAS-No. 1332-58-7 | |
| Hardener | SHOWA DENKO K. K. | • Gelation Time : 19 min |
| Unsaturated Polyester Resin (UP) | Srider BP-1055 (Lot. KE 624PL01) | • Optimum Hardening Time : 33 min • Maximum Heat-generating Temperature : 138°C |
| Methyl Ethyl Ketone Peroxide (MEKP) | NOF CORPORATION | • Hardener |
| Cobalt Naphtenate | CAS-No. 1338-23-4 | • Specific Gravity : 1.146 g/ml at 20°C |
| | Sigma-Aldrich Japan | • Accelerator |
| | CAS-No. 61789-51-3 | • Specific Gravity : 0.921 g/ml at 25°C |

Commonly, most of the raw materials for synthesis of polyester resins, typically referred to as UP, are derived from coal and petroleum (Fig. 2.1). The UP is one of the most widely used thermosetting resins for their excellent mechanical properties and simple processing (Osaman, E.A. Vakhguelt, A. Sbarski, I. & Mutasher, S.A., 2012; Chiu, H.T. Jeng, R.E. & Chung, J.S., 2004). However, due to high cross-link density of the UP and long-chain molecules formed from the polymerization of a monomer with a pre-polymer that have several C=C bonds, during the curing system, they come to be stiff and brittle (Albdiry, M.T. & Yousif, B.F., 2013).

Therefore, the UP is mainly used in its liquid state to make composites and needs additive to be cured to solid state. The additives used in the current work were of two types, viz. an accelerator cobalt naphthenate, and a hardner methyl ethyl ketone peroxide (MEKP).

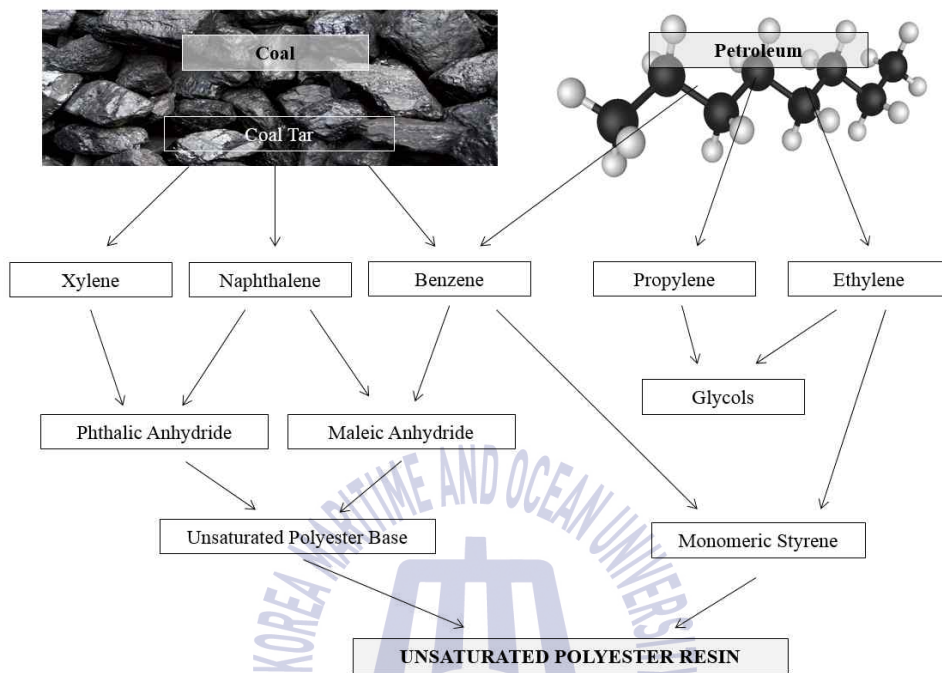
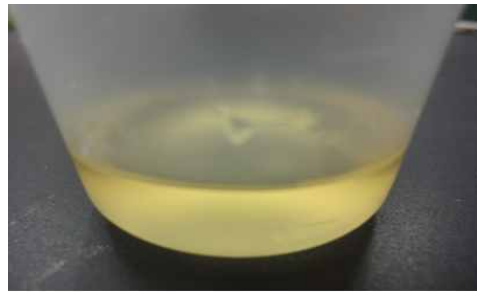
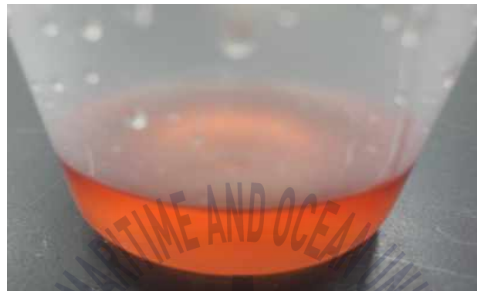


Fig. 2.1 Manufacture of polyester resins based on coal and petroleum

Fig. 2.2 shows the UP and the additives used in the present work. The proportion of additives used was 1 wt.% of UP. The accelerator and hardener were used in the ratio 1:1. The UP was formed by condensation reaction and cured with an accelerator and hardener to form cross-linked chains. Therefore, UP is a polyester that have been 'cured', i.e. treated with a monomer that lead to the chains to crosslink. Such cross-linking through curing resulted in a material, which was hard and durable, and will not melt on heating, i.e. a thermosetting resin.



(a) Unsaturated Polyester Resin (UP)



(b) UP + Cobalt Naphthenate



(c) UP + Cobalt Naphthenate + Methyl Ethyl Ketone Peroxide (MEKP)

Fig. 2.2 Matrix and addition

The HNT reinforcement has a hollow tubular shape. As shown in Fig. 2.3, HNTs have the following characteristics: the external surface of HNT is composed of siloxane groups (Si-O-Si), and the internal surface of HNT consists of aluminum hydroxide groups (Al-OH) (Joo, Y.H. et al., 2013). Most of HNTs have multi-wall structure (Jia, Z.X. et al., 2009). The length of the HNT varies from $100\text{ nm} - 3\text{ }\mu\text{m}$, the inner lumen

diameter is $10 - 30 \text{ nm}$ and the external diameter ranges from $30 - 150 \text{ nm}$. The actual chemical structure of the HNT used in this study is shown in Fig. 2.4.



Fig. 2.3 HNTs at room temperature

The contents of HNTs in the composites were 0.5, 1 and 3 wt.%.

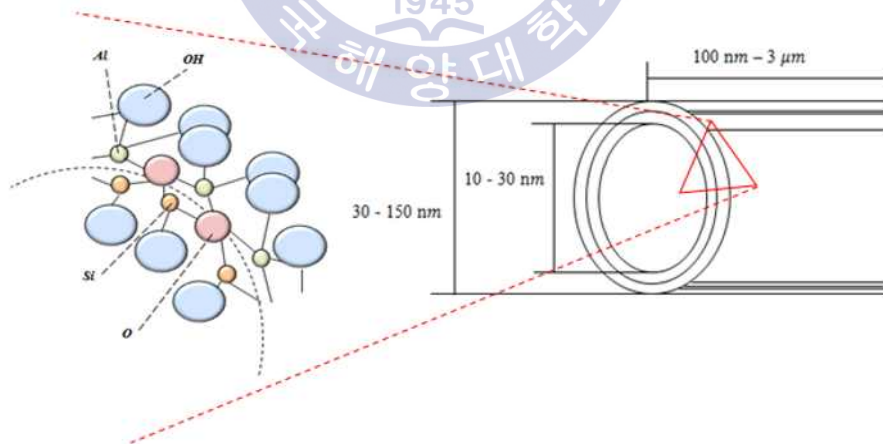


Fig. 2.4 Chemical structure of HNT

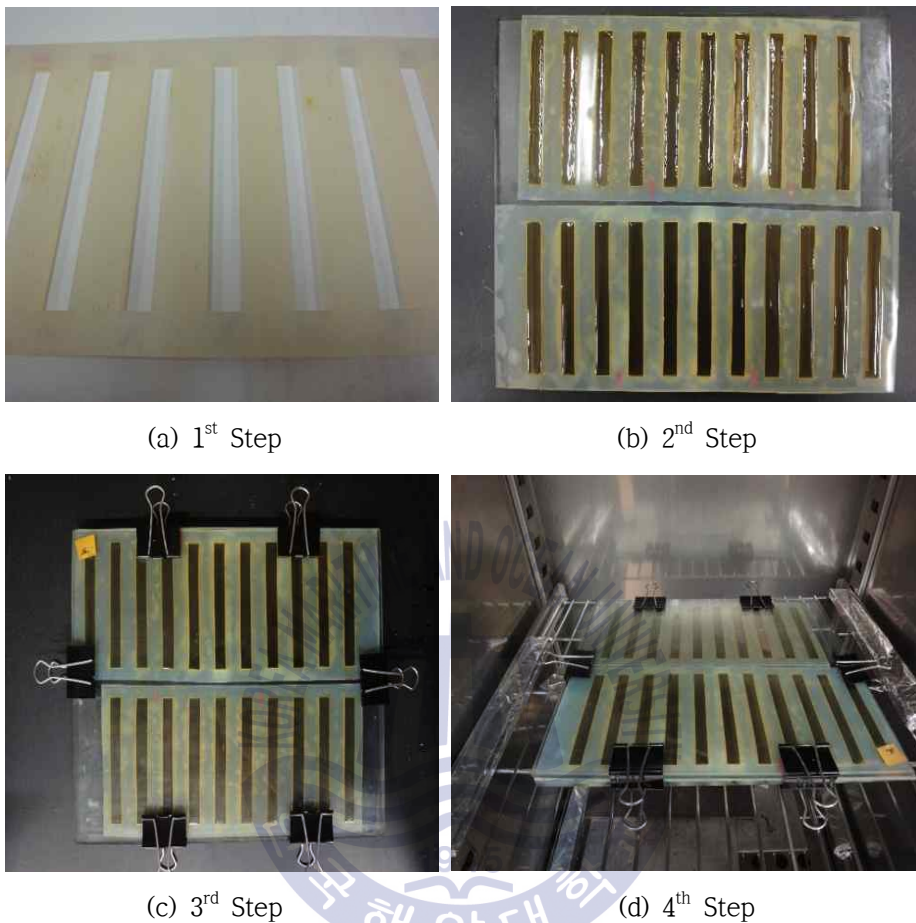
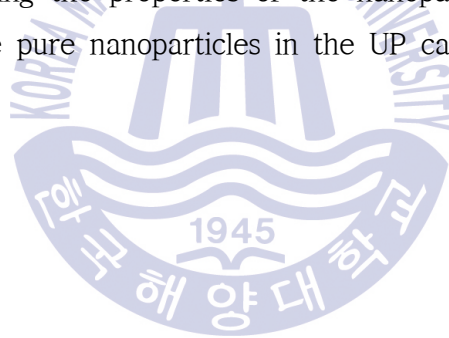


Fig. 2.5 Sample preparation procedure

The manufacturing method of the sample was divided into 4 steps, as shown in Fig. 2.5. Glass plates were used to support a fixed silicon mold on top and bottom. First the silicon plate is put on a glass plate. Next, the UP/HNT colloidal solution of the same amount was injected into each slot of the silicon mold using a dropping pipet. After the primary cure

of UP/HNT colloidal solution progressed, the upper part of silicon mold was covered with a glass plate such that the silicon mold was sandwiched by the glass plate and clamped. Next, it was put in a drying oven at 120°C to cure for 3 h. Although the optimum setting time of the UP is specified as 30 min, all samples required respectively different real times for complete curing the time.

Figure 2.6 shows the schematic diagram of the wadding process for manufacturing samples. The UP/HNT colloidal solution was left under the conditions of blocked air, so to avoid secondary reaction with air on the sample's surface, thereby maintaining samples with smooth surface. This condition such as anaerobic state also prevents any dust or foreign particles from altering the properties of the nanoparticles in the UP, so that the role of the pure nanoparticles in the UP can be evaluated.



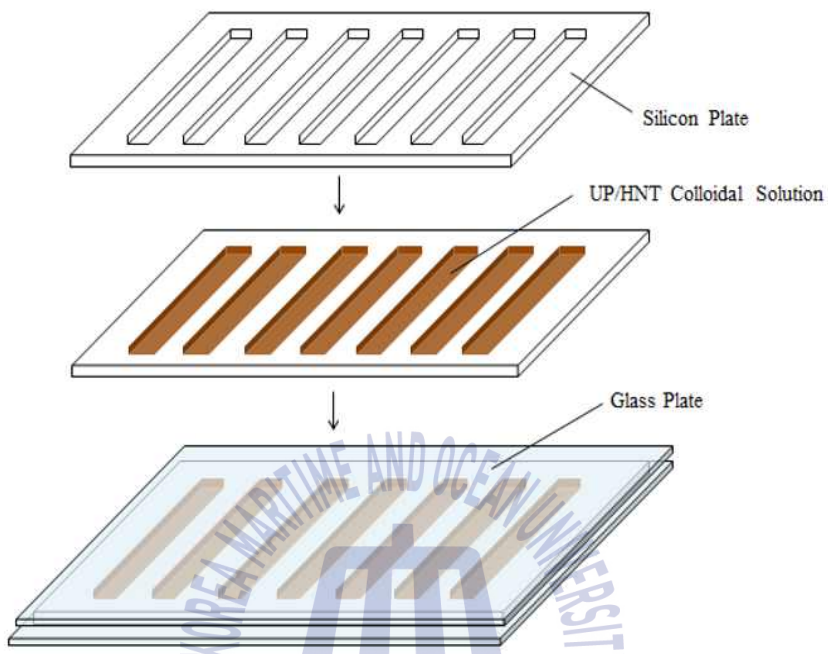


Fig. 2.6 Schematic diagram of resin infusion and shape preservation

2.1.2 Heat Treatment of HNTs at Different Temperatures

The HNTs used in this study were treated by heat using a heat controller (model SU02-110, CHINO Ltd.) under Ar gas (SHIKOKU ASECHIREN Ltd.) (Fig. 2.7). Preheating time of the heat controller was 30–40 min. and the processing time of heat treatment was set to 4 h and then, cooling of heat-treated HNTs for 1 h. The heat-treated HNTs

used in this study were classified into 4 groups according to their heat treatment temperatures. They were untreated HNT (UTHNT), 300°C (300HTHNT), 500°C (500HTHNT), 700°C (700HTHNT) and 1000°C (1000HTHNT) heat-treated HNT.



Fig. 2.7 Heat treatment machine

Fig. 2.8 shows the process diagram of heat treatment using the following steps:

- ① 10.0g of HNT powder was calcined at a certain temperature for 4h.
- ② Cooled to room temperature in a desiccator.

The current study was done at 5 different heat treatment temperatures. Additionally, the mechanical behaviors of the HNTs were compared at both less and greater than 500°C.

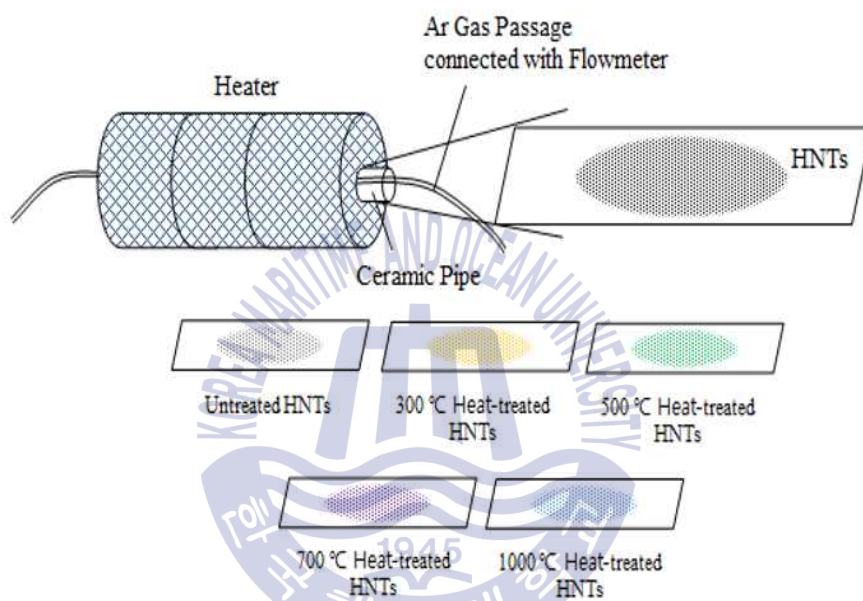


Fig. 2.8 Process diagram of heat treatment

2.1.3 HNT Dispersion by Ultrasonic Homogenization

In the current work, the parameters of ultrasonic homogenization considered were applied output power, operating time and volume of the sample. Fig. 2.9 shows a picture of the sonotrode. The operating time and the volume of the sample were kept at a fixed value, viz. 300 sec. and 18 ml, respectively. To examine the effects of the output power on effective dispersion of nanoparticles under same conditions, the output power values used were 45W and 60W (Table 2.2). The ultrasonic distribution inside the sample was of considerable importance. Since ultrasonic intensity decreases with distance from the emitting surface, close ranges were preferred, and when the volume of the sample is small, the distance from the sonotrode should be closer (Hielscher, T., 2005).



Fig. 2.9 Ultrasonic homogenization machine

Table 2.2 Conditions of ultrasonic homogenization used

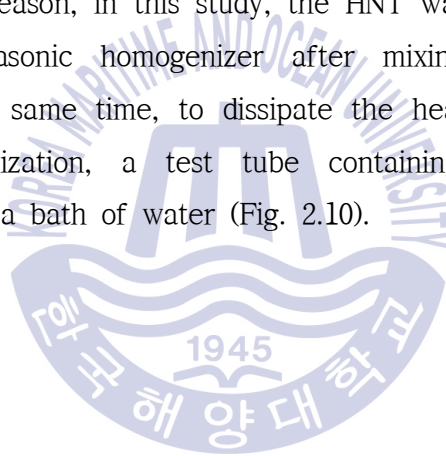
| | | | |
|---|--|--|--------------------|
| Product Name | ULTRASONIC HOMOGENIZER UH-150 | | |
| Manufacturer | SMT Co., Ltd. Japan | | |
| Experiment Condition | | | |
| Volume of the Sample (Use of Capacity) | Resin | 18 ml of Unsaturated Polyester Resin | |
| | Accelerator | 1 wt.% Cobalt Naphthenate | |
| | Hardener | 1 wt.% Methyl Ethyl Ketone Peroxide (MEKP) | |
| Temperature | Inner Tube for Resin | 44 - 49°C (Starting Point: 24 -27°C) | |
| Change of the Sample | Outer Tube for Cooling | 37 - 39°C (Starting Point: 24 -26°C) | |
| Operating Time | 300 sec. | | |
| Input Power | 150 W | | |
| Energy Purse | Pulsed at 80 % (Energy Pulse Lasted 0.8 sec. | | |
| Operation Type | Output Power | 45 W | |
| | Nanoparticle Addition | 0.5 wt.% | 1 wt.% 3 wt.% |
| | Output Power | 60 W | |

Another point to consider is that when the output power energy was delivered to the sample, a lot of heat was generated. The amount of heat generated depended on the output power.

If the temperature of the sample is raised due to heat generation, the rheological property, such as viscosity, of the sample is changed. In particular, it has a significant effect on the movement of the nanoparticles. Furthermore, the polymer resin contained nanoparticles under a high temperature means that the colloidal solution has a difference condition in the curing process. Curing of a resin has a close relation to the temperature. Typically, curing is promoted below the glass transition temperature (T_g). When T_g is reached, gelation proceeds quickly, at this time, it is not hardened.

For UP, the two additives that are required in final curing are curing agent (i.e. hardener) and curing accelerator. In this study, the additives were added in a definite order because in addition to HNT as filler it was also added as a reinforcement material. The resin was first mixed with the accelerator before the addition of HNT to prevent any pre-bonding between the accelerator and the HNTs. If the accelerator was impregnated into the HNT, a combination of the UP with HNT would not occur smoothly.

That is, to achieving proper stirring process, a different energy is required. For this reason, in this study, the HNT was dispersed into the resin by the ultrasonic homogenizer after mixing of UP and the accelerator. At the same time, to dissipate the heat generated by the ultrasonic homogenization, a test tube containing UP/HNT colloidal solution was put in a bath of water (Fig. 2.10).



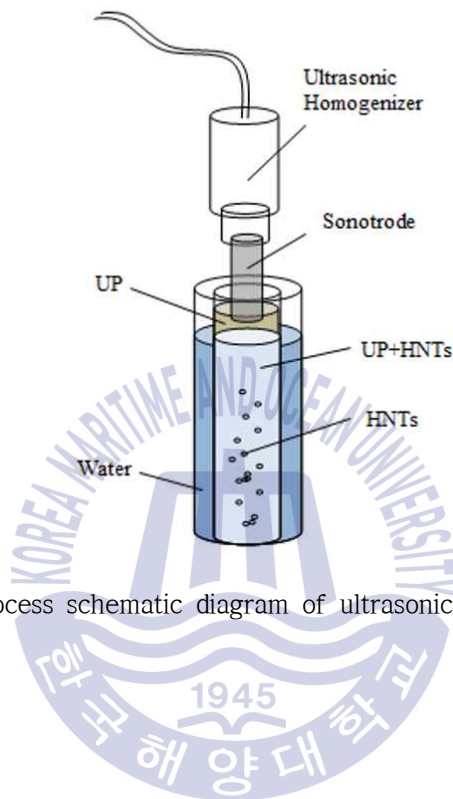


Fig. 2.10 Process schematic diagram of ultrasonic homogenization

2.2 Characterization of UP/HNT Nanocomposites

2.2.1 X-ray Diffraction

XRD analysis is a non-destructive analytical method and is used to obtain the crystal structure and chemical composition of a sample. XRD also indicates the size of the constituent material. XRD is the quantitative (element content) analysis of the components by measuring the respective intensity of diffracted ray. If the crystal structure and compound type of the material are different, the form of a diffraction

pattern changes.

In this study, the XRD patterns were recorded on a multiflex (Rigaku Corporation) with Ni filter and CuK α radiation ($\lambda=0.154$ nm) generated at 40 kV and 40 mA. The scan rate was $1^\circ 2\theta/\text{min}$. X-ray peaks were observed in the range of $10^\circ 2\theta$ to $70^\circ 2\theta$. This is to be attributed to crystallographic properties of the nanoparticle. The background knowledge of this angle range is as follows: by observing a crystallographic change and chemical structure of the heat-treated HNTs, structural changes of the HNTs in the actual phenomenon were demonstrated.

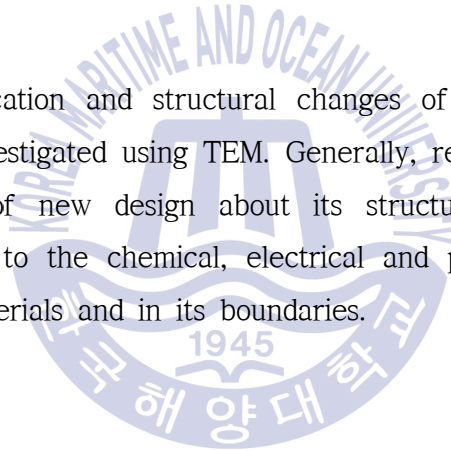
Generally grain size of the nanocrystalline material cannot have a substructure because it is too small at a size of 10 to 100 nm. The x-ray diffraction pattern is formed of a series of concentric rings having the same center. Each of the rings signifies diffraction from the respective surface of a crystal. To note, if the grain size is larger than about $10 \mu\text{m}$, the diffraction rings from the X-ray-irradiated area of the specimen will show as discontinuous points. The grain is enough to make the shape of concentric rings in the size between 500 to 10,000 nm. The size refers to the ideal grain size. If the grain size is small, 500 to 100 nm, the width of the diffraction ring becomes larger.

However, if the grain size is much smaller than 100 nm, the diffraction will occur only in a very low angle without creating diffracting ring because the volume under x-ray illumination is too small. Thus, the size of HNT used in this study was analyzed and a suitable angle was set for outer diameter of 30-150 nm and length of 100-3,000 nm.

2.2.2 Transmission Electron Microscopy (TEM)

In this study, structural changes in the surface of the HNTs, caused by heat treatment, were observed using a TEM (JEOL Ltd, model JEM-2100). The TEM gets an image through transmitted electrons by irradiating an electrons to the sample and by obtaining the image using the electron beam which is diffracted. It is used to analyze the crystal structure of the material (An, J.P. & Park, J.G., 2006). In order to observe nanocomposites, preferentially nanocomposites were cryogenically ultra-microtomed to 300 nm thickness (Pal, P.P. Kundu, M.K. Kalra, S. & Das, C.K., 2012).

The basic specification and structural changes of HNTs due to heat treatment were investigated using TEM. Generally, research for materials and development of new design about its structure depends on the knowledge relating to the chemical, electrical and physical prperties of the multi-layer materials and in its boundaries.



2.2.3 Impact Test

Impact test was carried out using an izod impact tester (YASUDA SEIKI SEISAKUSHO, LTD., No. 12353) (Fig. 2.11-(a)). The impact strength was calculated from unnotched specimens hit at half specimen's the length (following JIS K 7062). The impact specimens produced had final dimensions of 80.0 mm x 10.0 mm x 4.0 mm (length x width x thickness) and at least four specimens were made for each specimen fabrication condition (Fig. 2.11-(b), (c)). At first, the corrected energy (E_c , J) was measured from the angle point reached by the hammer after breaking the specimen (β). The impact strength was calculated from the formula (1).

$$E_c = WR[(\cos\beta - \cos\alpha) - (\cos\alpha' - \cos\alpha)\left(\frac{\alpha + \beta}{\alpha + \alpha'}\right)] \quad (1)$$

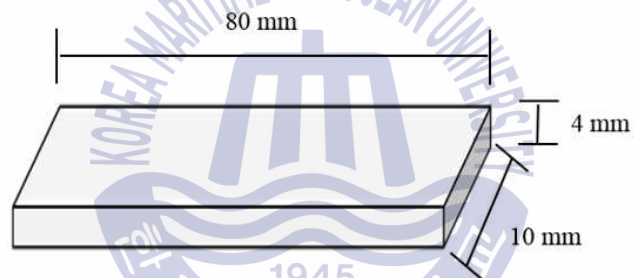
Where, WR is the moment around the axle of the hammer (2.949040 N · m), α is the initial lift angle of the hammer (150.0°C) and α' is the real lift angle of the hammer (148.4°C). The izod impact strength (a_{iU} , KJ/m²) of unnotched specimens was calculated using equation (2):

$$a_{iU} = \frac{E_c \times 10^3}{b \times h} \quad (2)$$

Where, h is the thickness (mm) and b is the width (mm) of the test specimen. The test was set at 5.5 J of hammer' s work.



(a) Izod impact test machine



(b) Impact test specimen according to JIS K 7062



(c) Manufacturing mold of silicon type and specimen

Fig. 2.11 Equipment used for impact test and the samples

2.2.4 Tensile Test

Tensile test was performed to evaluate the mechanical property of nanocomposites based on UP/HNTs. The test speed was 1.00mm/min at room temperature under the condition of JIS K 7055 by Universal Test Machine from Kyung-do Corporation (KDMT-156). The machine is shown in fig. 2.12. Tensile strength represents maximum tensile load divided by specimen' s cross sectional area.

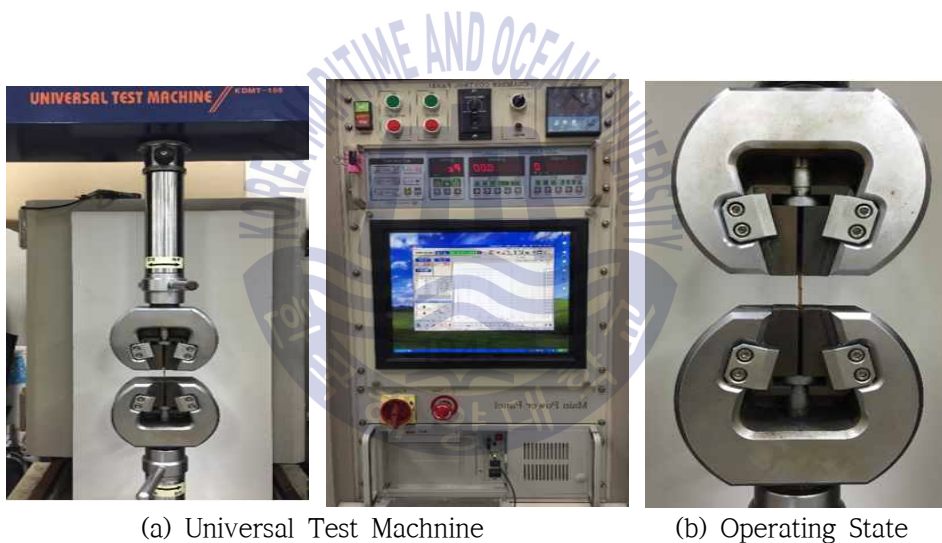
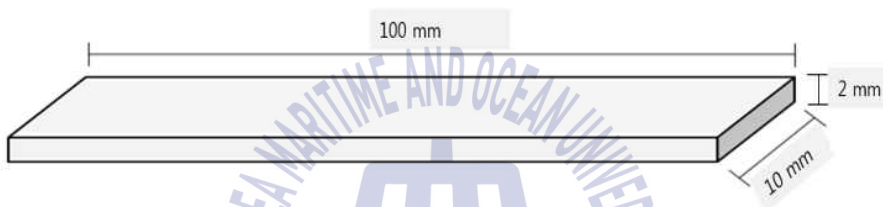


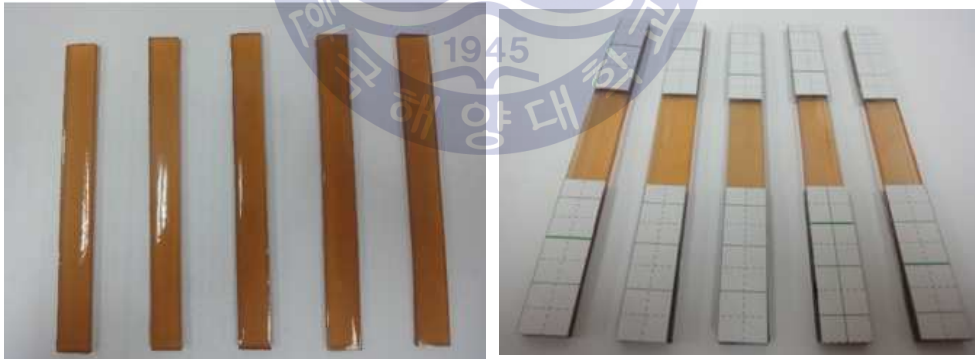
Fig. 2.12 Machine for tensile test

The specimen dimensions were 100 mm x 10 mm x 2 mm (length x width x thickness) (Fig. 2.13) and the gage length was 50.00 mm. The tensile test is the most basic method for the analysis of mechanical properties of a material.

In addition, instead of dog-bone or dumbbell-shaped specimens, coupon specimens attached with paper tabs were used in this study. This specimen has the disadvantage that unlike dog-bone-shaped specimens it is hard to fracture at the same location. However when fixing the specimen in a tensile machine, by the tab between the tensile machine and specimen, it prevents slippage and can get accurate test results.



(a) Schematic diagram of tensile test specimen followed JIS K 7055



(b) Specimens for tensile test

Fig. 2.13 Samples for tensile test

Since composites with a polymer matrix is highly brittle, the external stress applied to the specimen in a tensile machine can cause damage to the specimen. In other words, the tab prevents damage of the specimen in a specific direction. By reinforcing by the tab, damage of the specimen can be prevented. That is, the decision of the appropriate type of the specimen in accordance with the materials is a very important factor because it is more likely the creation of defects or stress concentrating.



Chapter 3 Results and Discussion

3.1 Observation of Structural Changes by X-ray Diffraction and TEM Imaging

X-ray diffraction (XRD) analysis of HNTs at different heat-treatment temperatures showed the structural change of the HNTs as the heat treatment temperature increased. As shown in Fig. 3.1, a mixture of HNT-7 Å and quartz or silicon oxide was measured from UTHNT (untreated HNT) to 500HTHNT (500°C heat-treated HNT). For 700HTHNT (700°C heat-treated HNT) the HNT-7 Å was destroyed and it changed to a mixture of amorphous substances with quartz or silicon oxide. For 1000HTHNT (1000°C heat-treated HNT), amorphous or low crystallinity HNT was observed such as crystals of quartz or silicon oxide. So it can be estimated that temperature changed the crystal phase.

Smith et al. (Smith, M.E., Neal, G., Trigg, M.B. & Drennan, J., 1993) showed that the reaction scheme for the calcination of kaolinite initially involved dihydroxylation between 600°C and 850°C, where most of the OH groups were eliminated, causing reduced coordination of originally octahedral aluminum. A large exothermic situation at ~ 980 °C, thought to be triggered by elimination of the last hydroxyls, owes to the creation of a striking alumina-rich phase.

In XRD peak, 12.30° and 24.85° represents the typical diffraction peaks of HNT. When the temperature changed from 25°C to 400°C, the crystal structure of the HNT did not change any further by heat treatment. However, the crystal structure of the silicate layers were

broken forming an amorphous one due to dehydration and oxidation of aluminol groups at a higher heat treatment temperature of 500°C.

According to the recent research, the XRD peak of 1000HTHNT shows a reflection centered around $21.1^\circ 2\theta$ which is attributed to the dissociative amorphous SiO_2 that divides from the metahalloysite. And reflections corresponding to peak of around 36.5° ($d=0.240$ nm), 46.05° ($d=0.198$ nm) and 67.5° ($d=0.140$ nm) should impose to $\gamma\text{-Al}_2\text{O}_3$. The reflections assign to $\gamma\text{-Al}_2\text{O}_3$ are not present but those of mullite are well resolved over heat treatment temperature of 1200°C (Yuan, P. et al, 2012).

Therefore, the temperature of 500°C had a significant impact on the crystal structure of the HNT. In particular, 26.62° highly likely relates to quartz and the basic reflection of 26.62° was observed and is unaffected by the temperature. In 1000HTHNT, mullite was observed, which led us to think that it was formed around 950°C. There is a possibility that it was partially cristobalite. Furthermore, the peak of the 1000HTHNT did not correspond to the original peak of HNT, and the mullite or SiO_2 was created in the peak of 26.62° . The peak at 46.05° indicated formation of aluminum oxide.

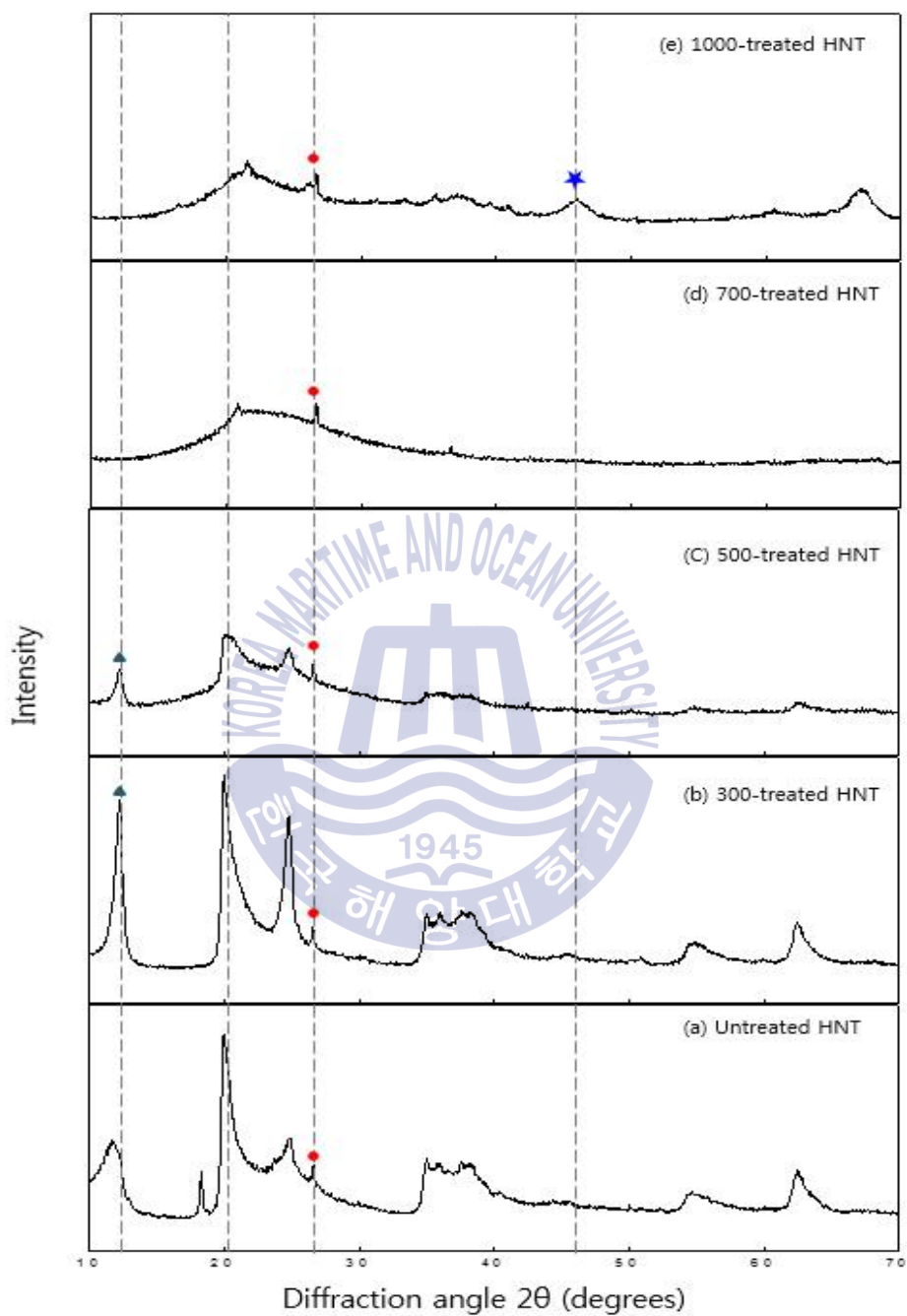


Fig. 3.1 X-ray observation of HNTs at various heat treatment temperatures

TEM analysis (Fig. 3.2) showed that HNT in all cases had a tubular structure in common and formed aggregates. For the case of heat-treated HNT, the HNT showed broken or bent shapes and formed clusters. The surface of the heat-treated HNTs at high temperature was not smooth and had rough spots.

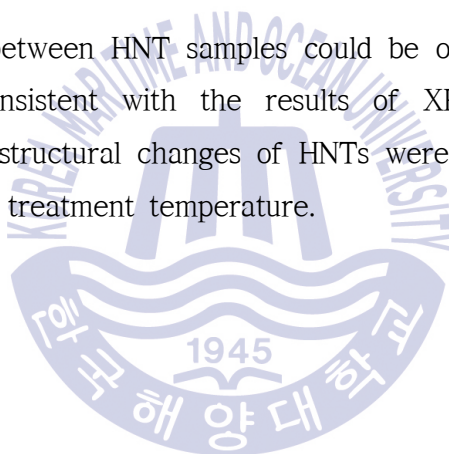
In general, functionalization of HNT introduces many useful characteristics in HNT. Furthermore, heat treatment can eliminate any physically bounded water, break the structure of water through dihydroxylation of the aluminol groups in the HNT structure and result in a structural rearrangement of HNT, which correspondingly changes the pore structure and surface characteristics (S.Kadi, et al, 2012 cited in Q. Wang, J. Zhang, Y. Zheng & A. Wang).

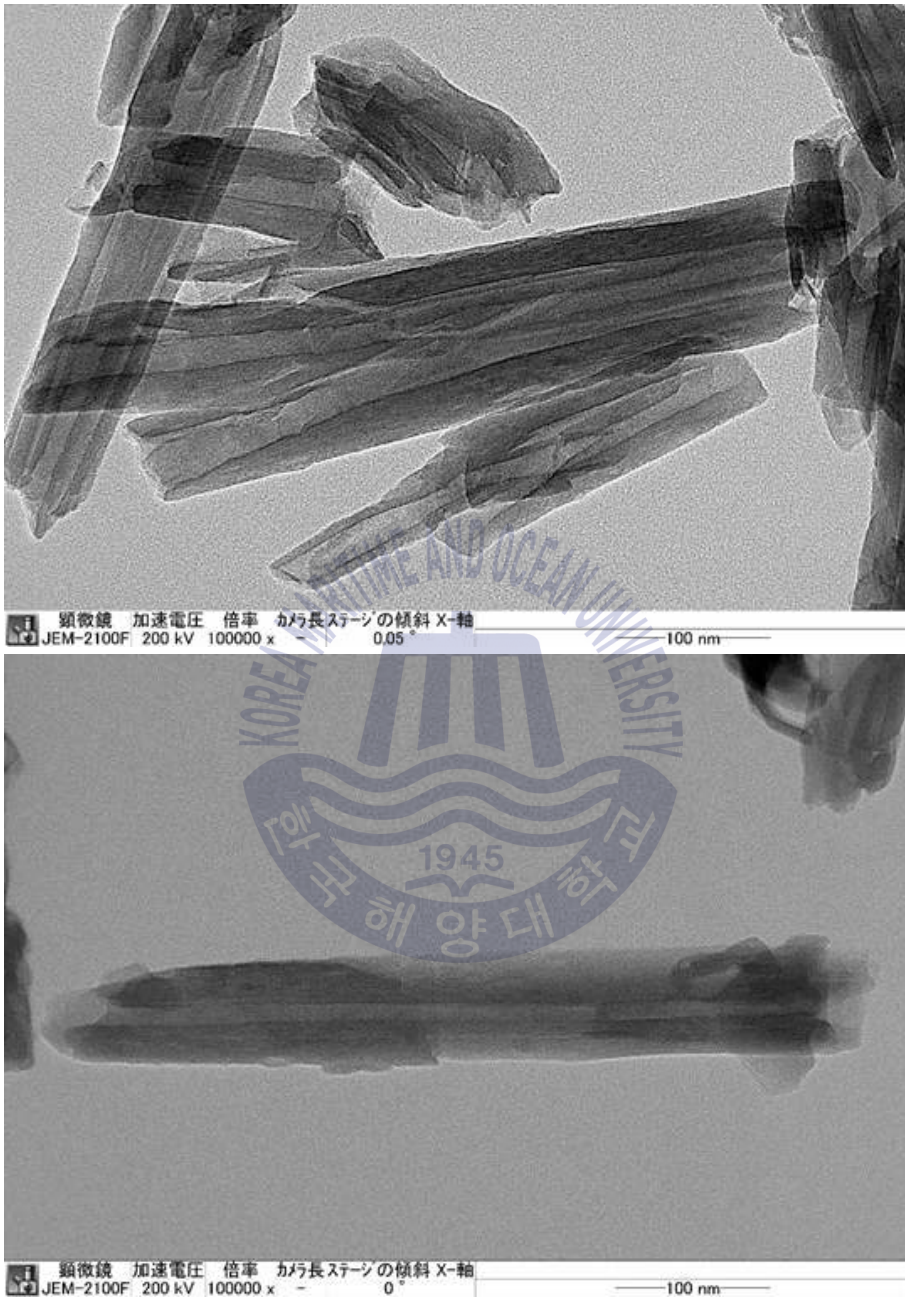
Herein, heat treatment time was invariant. However, heat treatment temperature was used as an independent variable with various values and by setting the number of variables, the effect of heat-treated on HNTs was observed. Past research suggested that the crystal structure of HNT is retained when the temperature is less than 400°C, but HNT becomes amorphous owing to the dehydroxylation of structural aluminol groups when the temperature is up to 500°C. On the other hand, the tubular structure is still the same such as the untreated HNT (Q. Wang, J. Zhang, Y. Zheng & A. Wang, 2014).

No significant difference in shape was observed between HNTs in Fig. 3.2-(c,d) and (a), however, in Fig. 3.2-(c,d) they had more uneven surface than in Fig. 3.2-(b). No amorphous structure was observed, such as aluminum silicate in Fig. 3.2-(c). Destruction of the HNT layered structure occurred at 500°C and the layered structure of the HNT have been partially unified by dehydration phenomenon. According to past

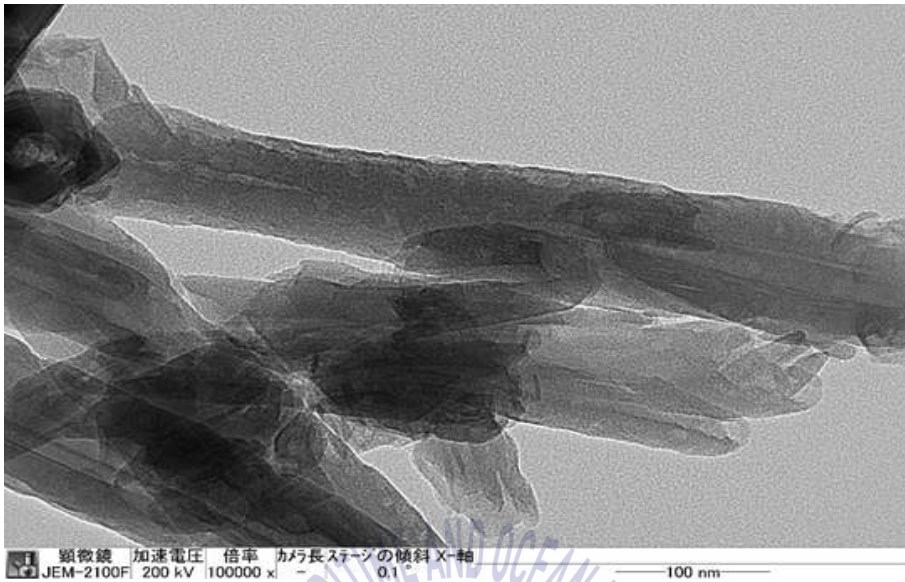
research, heating at 120 °C caused conversion of HNTs to 7Å of HNTs through loss of the water from the interlayers (Yuan, P. et al, 2012). At 1000°C, as shown in Fig. 3.2-(e), the silicate-layered structure of the HNT was destroyed. The unevenness of several nanometers on the surface was observed distinctly. Also no formation of a bi-layered hollow tubular structure of HNT was observed. In addition, the HNTs formed clusters with structural destruction and was observed at room temperature in a state of agglomeration. The size of particles also became relatively small (shrinkage phenomenon) due to structural rearrangement.

The differences between HNT samples could be observed through the TEM and were consistent with the results of XRD analysis. It was concluded that the structural changes of HNTs were caused by chemical change due to heat treatment temperature.

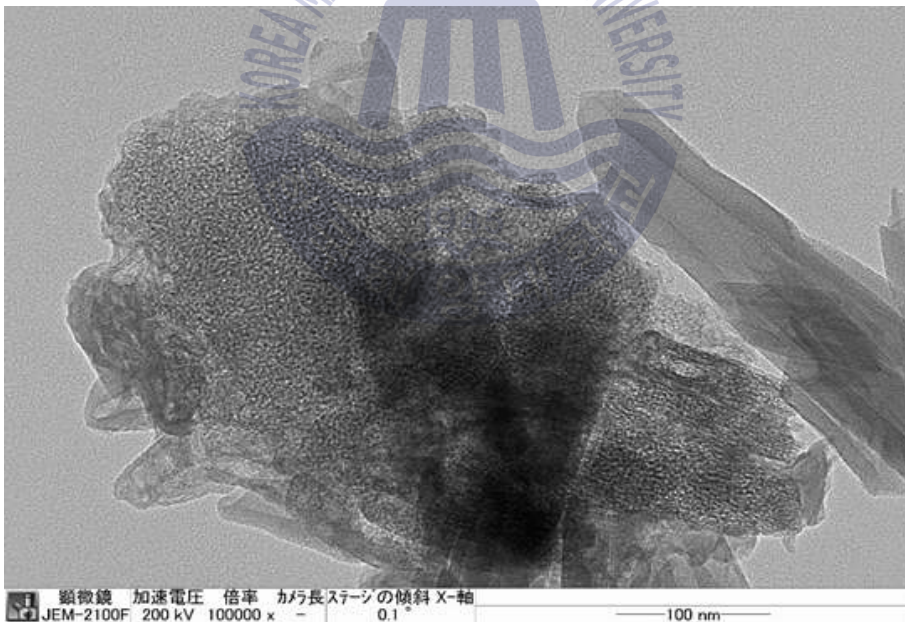




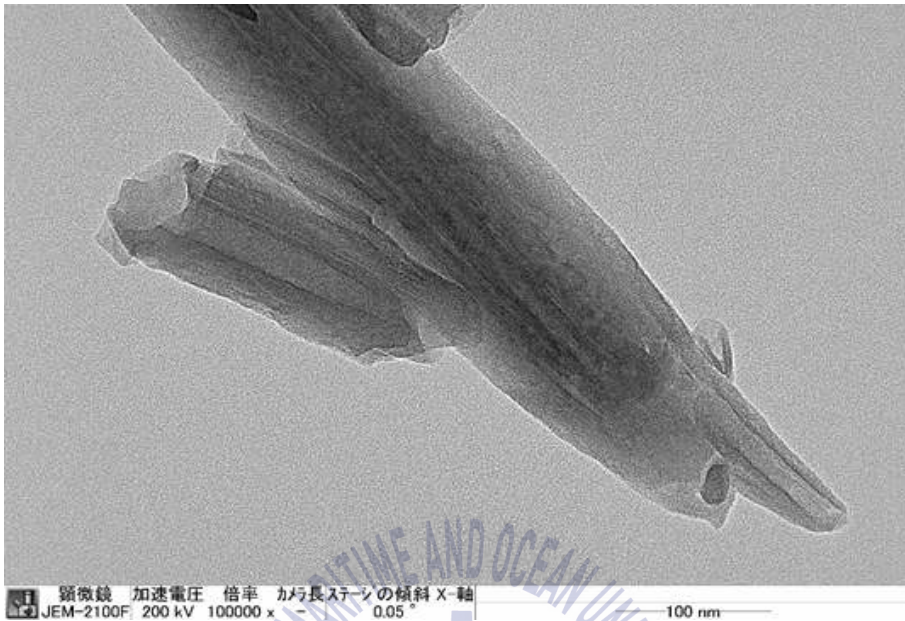
(a) UTHNT (untreated HNT)



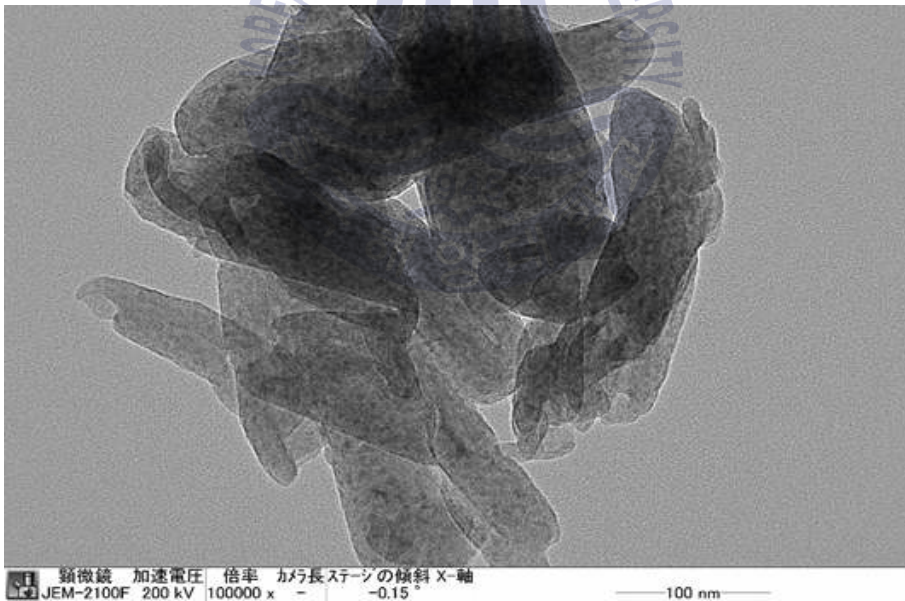
(b) 300HTHNT (300°C heat-treated HNT)



(c) 500HTHNT (500°C heat-treated HNT)



(d) 700HTHNT (700°C heat-treated HNT)



(e) 1000HTHNT (1000°C heat-treated HNT)

Fig. 3.2 TEM of HNTs at various temperatures

3.2 Changes in Mechanical Properties

3.2.1 Impact Properties

To obtain optimized physical properties of heat-treated HNTs at various temperatures and UP nanocomposites, the output power of the ultrasonic homogenizer was set as a variable. By observing the impact behavior of nanocomposites containing dispersed HNTs at 45W and 60W, the dispersion conditions were optimized for the heat-treated HNTs.

Figure 3.3 shows the results of impact test performed to evaluate the effect of heat-treated HNTs and UP under 45W of ultrasonic homogenization. We preferentially compared only the impact strength between UP and its nanocomposites. When considering an error range, the samples showing the ideal strength were the nanocomposites containing 1 wt.% of 1000HTHNTs. Usually, as the size of particles increases, fracture toughness and elastic modulus increase, but strength decreases. Furthermore, the rheological property of resin is changed by nanoparticles. Therefore, the research for optimal dispersion of nanoparticles in resin is necessary to evaluate the reinforcing effects of HNT from the viewpoint of resin viscosity and dispersion of nanoparticles (Park, J.H. & Kim, J.Y., 2002).

Looking at heat-treated HNTs at various temperatures, UTHNT nanocomposites showed the lowest impact strength. As the heat treatment temperature increased, strength tended to increase. The heat-treated HNT at high temperature showed a severe structural change. The layer structure was destroyed and the shape changed to the single-layer tubes, indicating that the HNT with the layer structure did not smoothly couple with UP. This implies heat treatment on HNTs is

required to realize a reinforcing effect.

Comparing between contents of HNTs, overall it did not show any specific trend. For UTHNTs and 300HNTs, the UTHNT showed a significantly lower strength than 300HNT. This can be considered as a typical example of a reverse reaction about the basic reinforcing effect of HNTs. It showed better reinforcing effects when 1 wt.% of HNT was added, as seen for 500HNT and 1000HNT. However, 3 wt.% addition of HNT showed a negative effect on reinforcement.

The above observations were due to particle properties of the nanoparticles. The limitation of nanoparticles is aggregation. Due to cluster formation, it was difficult to form a homogeneous dispersion of nanoparticles in the UP. These HNTs aggregated to achieve the spatial equilibrium in UP when exceed the appropriate addition amount. Also, re-aggregation of HNTs occurs over time after dispersion. That is, the nanoparticles in nanocomposites results in diminution of strength phenomenon instead of reinforcement effects due to the action as pore groups of aggregation.

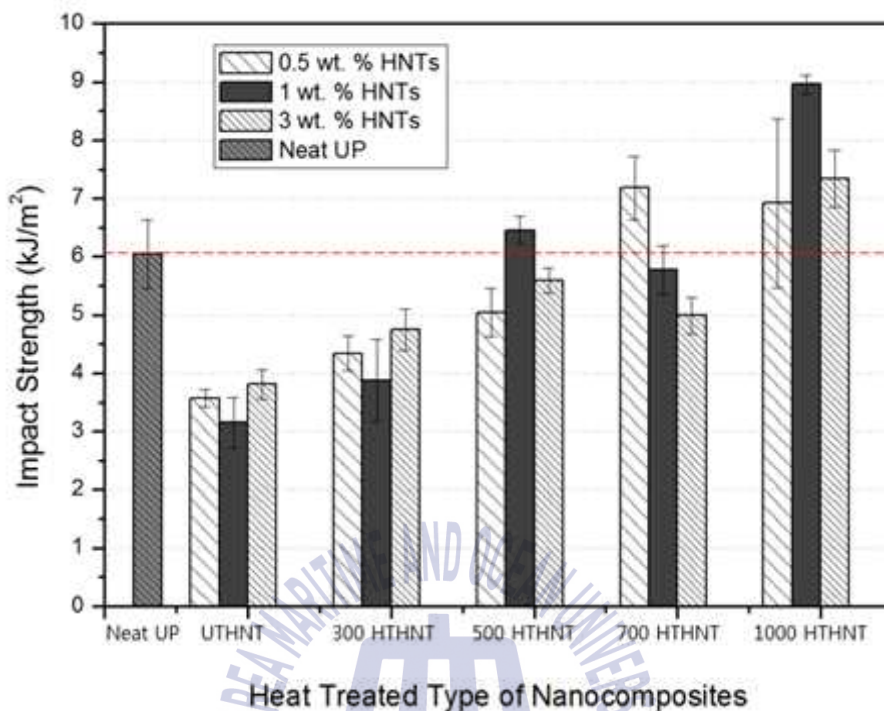


Fig. 3.3 Comparison of impact strength of neat UP and its nanocomposites under 45W of ultrasonic homogenization condition

Fig. 3.4 is a graph showing the effect of impact reinforcement when the output power was set to 60W in the UP/HNT colloidal solution. Overall, the nanocomposites showed similar impact strength as that of neat UP, except 1000HTHNTs. In particular, the 700HTHNTs showed a significantly high reinforcement effect and generally, the reinforcing effect was greater in every case when 1 wt.% HNTs was added to the UP. The impact strength of 3 wt.% HNTs was similar to UP than 0.5 wt.% HNTs nanocomposites. However, this numerical value was rather lower compared to the 1 wt.% HNTs nanocomposites.

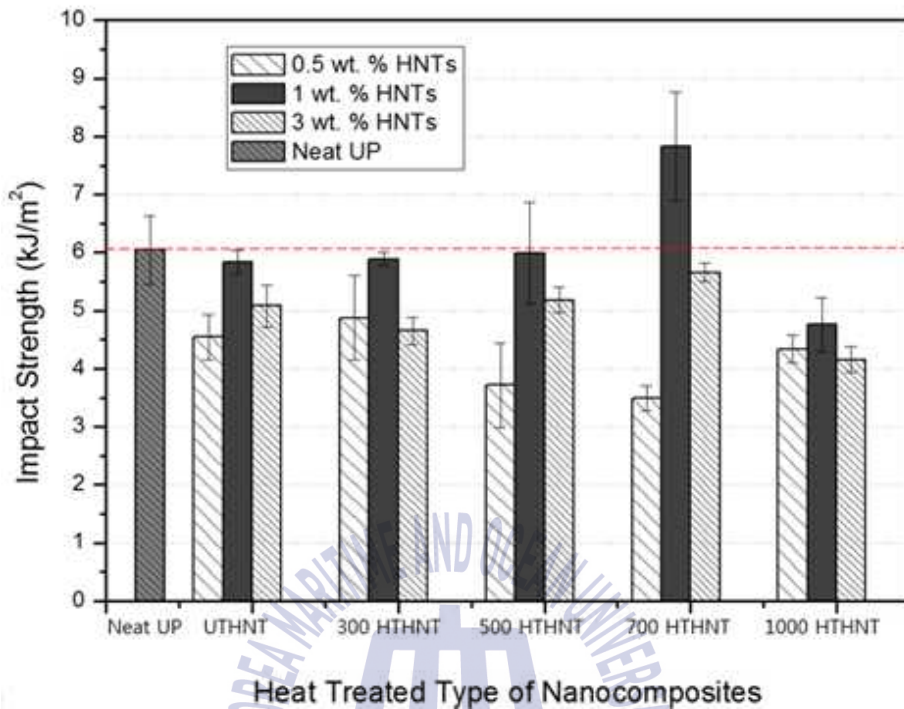


Fig. 3.4 Comparison of impact strength of neat UP and its nanocomposites under 60W of ultrasonic homogenization condition

In fact, the largest difference with 45W and 60W is the size of the nanoparticles. The ultrasound is generated by the cavitation of bubbles while propagating through UP/HNTs colloidal solution. The generated bubbles transmitted force to HNTs within the UP and collapsing at the same time due to pressure difference. The bubble explosion was affected by the power, such as 45W and 60W and the homogeneity of the dispersion was also affected depending on the strength of the power. Therefore, in general, the homogeneity is increased by using larger force and the reinforcing effect of HNTs is revealed more

clearly. In other words, impact strength behavior and its tendency in both cases should be the same. It can be expected that the reinforcement effect will appear more clearly for 60W power.

In practice, however, the reinforcement effect was more pronounced for HNTs up to 500HTHNT nanocomposites. For 700HTHNTs and 1000HTHNTs, the impact strength was reduced. Especially, for 1000HTHNT, it has a very large difference in strength. The reason is that due to heat treatment the structural strength of HNTs decreased and structural detachment was observed. As a result, the HNTs did not smoothly bond with UP. Appropriate power of ultrasonic homogenizer improved the dispersion of nanoparticles in the matrix. However, a high power affected the unique properties of the nanoparticles. High power also inhibited the original reinforcing effect of the nanoparticles. The content of HNTs was an important factor. The content of the 1 wt.% HNTs had the highest property but a small amount, say 0.5 wt.% HNTs acted as a defect rather than a reinforcing factor.

When more than 1 wt.% was added, the nanocomposites were influenced by the dispersion of nanoparticles and the reinforcing effect was also affected. The 1000HTHNT at 45W and the 700HTHNT at 60W showed quite high impact strength at 1 wt.% HNTs content. Therefore, the 1000HTHNT at 45W and 700HTHNT nanocomposites at 60W could be used when a high impact resistance is required.

3.2.2 Tensile Properties

A tensile test was also performed at room temperature as the basic evaluation method to find out the mechanical properties of the material. Generally, the tensile test is simple to operate and relatively inexpensive. The tensile test is to observe the reaction of the tension of the material by pulling it. Therefore in this study, when the material is pulled until failure the reaction of the UP/HNT nanocomposites for tensile strength were observed. The stress of the highest load point was calculated. After the heat-treated HNTs at various temperatures were dispersed in a matrix using ultrasonic homogenization, tensile test was carried out. From the values of tensile strength and the modulus of elasticity, which signifies the degree of strength of a material, the reinforcing behavior of the HNTs was evaluated.

Figure 3.5 shows the graph of tensile strength and modulus of elasticity of the UP/HNT nanocomposites prepared by an ultrasonic homogenizer at 45W of output power. Each of the nanocomposite materials showed a lower strength than the tensile strength of neat UP. However, 0.5 wt.% UTHNT and 0.5 wt.% HTHNT nanocomposites showed a similar strength with that of neat UP. Through this graph, a reinforcing effect of heat-treated HNTs could not be confirmed. In other words, when the external stress was applied to HNTs along the pulling direction, the HNTs showed no reinforcing effects in the UP matrix. Especially when the content of HNTs became high, reducing the strength was sharply increased.

Comparison of the modulus of elasticity revealed that the nanocomposites reinforced HNT were 2 times higher than the neat UP. That is, the strain of the nanocomposites reinforced HNT was lower

than the strain of the neat UP and it was considered that due to reinforcing of the UP by HNTs, the nanocomposites reinforced HNT became more brittle. By dispersing the HNT in the UP, the strength of the material was expected to improve. However, tensile tests showed that the HNT did not affect the reinforcing effect on the tensile force. It was estimated that the HNT acted as a defect instead of reinforcement when the external force acted in the longitudinal direction, since the rupture time was accelerated with an increasing amount of HNTs excluding content of 0.5 wt.%. Furthermore, by heat treating the HNT, structural changes were observed due to dehydration. So heat treatment was likely to be a factor to decrease the coherence between the UP and HNTs. Particularly, heat treatment of HNTs up to 700°C had significant effect on bonding with polymer manifested as structural and chemical changes.

Therefore, considering variations in properties caused by agglomeration and structural destruction of HNTs, the nanocomposite with 0.5 wt.% 700HTHNT can be regarded as more superior material compared to traditional neat UP at 45W of ultrasonic output homogenization. This result was based on the tensile strength and modulus of elasticity.

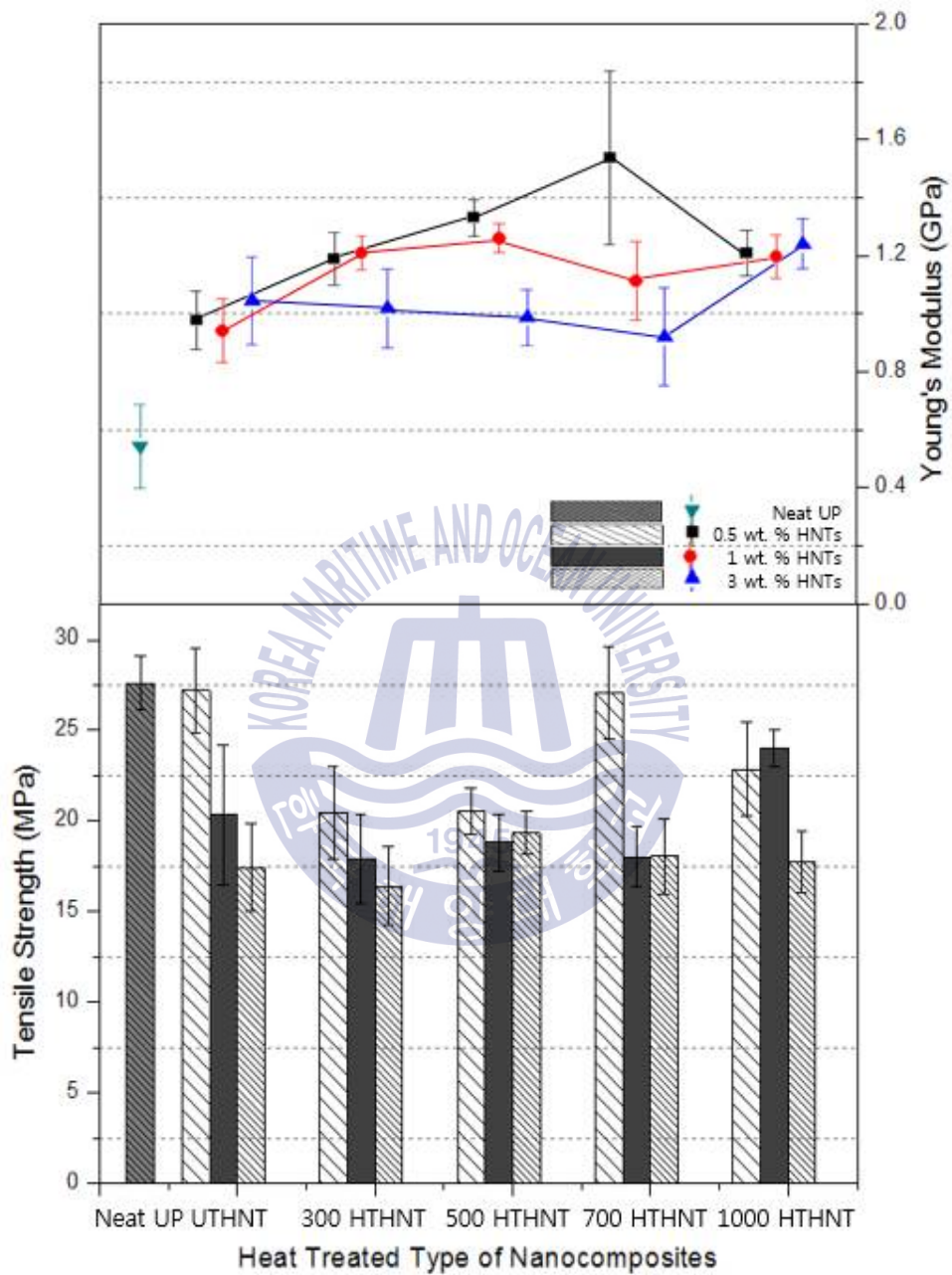


Fig. 3.5 Results of tensile test of neat UP and its nanocomposites under 45W of ultrasonic homogenization condition

Figure. 3.6 displays a graph showing the tensile strength and modulus of elasticity of the nanocomposites produced using 60W power of ultrasound. When compared between neat UP and the nanocomposites with HNT, the UP/HNT nanocomposites showed a much lower intensity with the exception of the nanocomposites with UTHNT. The heat-treated HNTs showed a relatively lower intensity in comparison with the test specimens using the 45W of ultrasonic wave as described above. This means that the ultrasonic intensity has a large influence on the inherent properties of the nanoparticles. Although ultrasonic wave was used to achieve uniform dispersion of the HNTs within the resin, it was found that ultrasound intensity was not proportional to uniformity in dispersion. When the ultrasound intensity was high, destruction and deformation of the nanoparticles occurred.

Therefore, the reinforcing effect along the tensile direction was very small. In other words, no distinct trend in the graph could be established. Nevertheless, 1 wt.% UTHNTs nanocomposites showed the highest tensile strength under current given conditions.

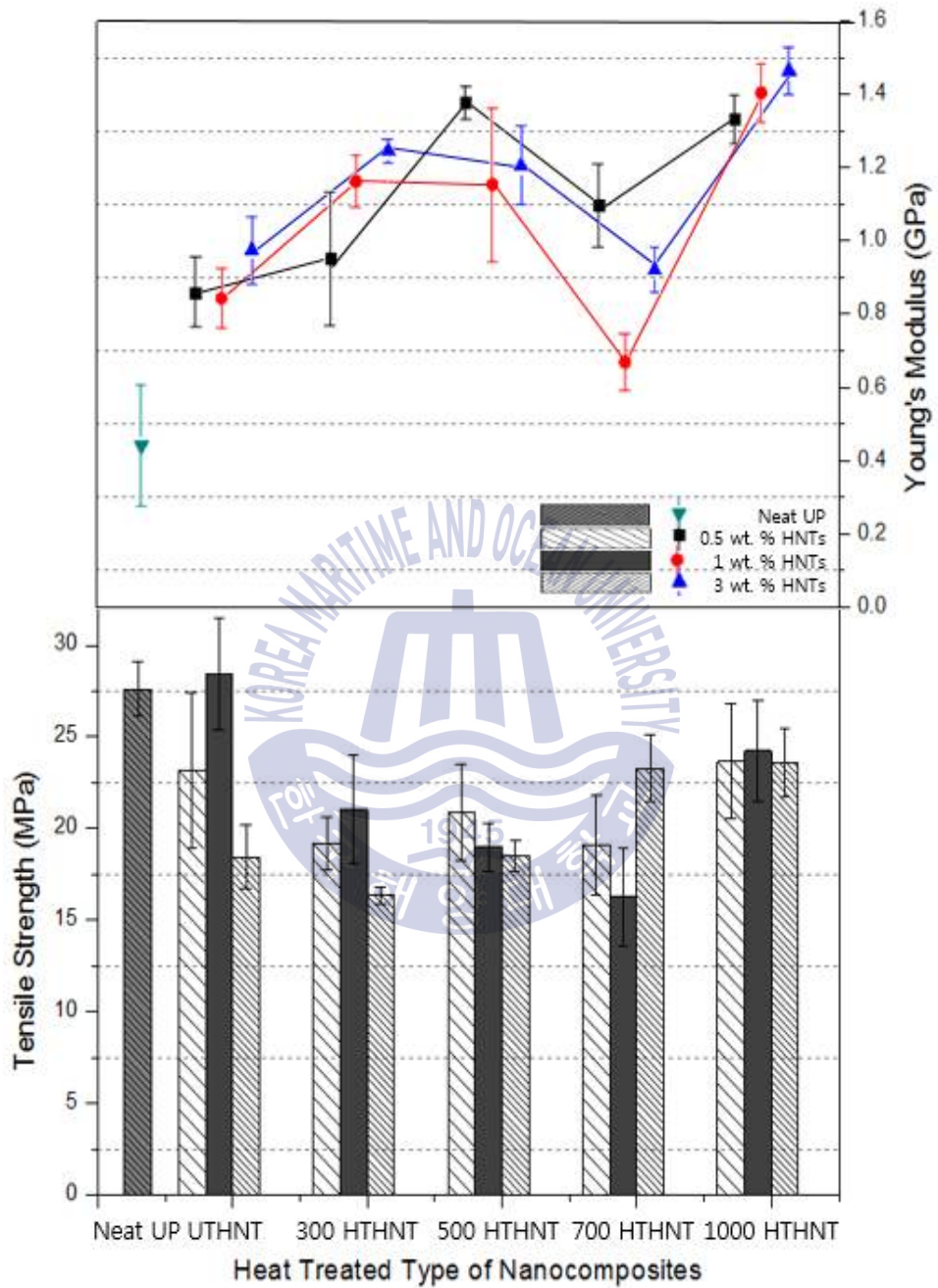


Fig. 3.6 Results of tensile test of neat UP and its nanocomposites under 60W of ultrasonic homogenization condition

3.2.3 Considerations on the Effects of Nanoparticle Dispersion on Mechanical Strength

To understand the effect of nanoparticles on the properties of nanocomposites, it is important to investigate the optimal dispersion properties of the nanoparticles. Especially, HNTs tend to agglomerate under the van der Waals force (Park, J.J. & Lee, J.Y., 2011). Result of preliminary research showed that certain amount of HNTs can noticeably increase the strength, modulus and fracture toughness of polymer matrix; however, achieving homogeneous dispersion of HNTs in some matrix remains a challenge owing to agglomeration of large particle clusters (S. Deng, J. Zhang & L. Ye, 2009).

Therefore, to achieve a uniform distribution of nanoparticles, in this study, the factors related to dispersion were optimized and suitable process environment for materials was established by dividing them into constants and variables. The methods of dispersion can be of various types, such as mechanical dispersion, ball mill homogenization, ultrasonic dispersion and electrical dispersion. Each of these methods has its own advantages and disadvantages. When nanoparticles are uniformly distributed within a polymer matrix and not present in an agglomerated state improved properties of the polymer resin can be achieved. Through ultrasonic homogenization, such homogeneous distribution of nanoparticles within a polymer can be easily obtained.

In other words, according to the advanced research, the most significant competitiveness of nanocomposites is that even if only a small amount is added, the improved results can be obtained with high characteristics. But, this is the possible conclusion when the nanoparticles are made of a complete detachment in the polymer resin

(Park, J.J & Lee, J.Y., 2011). The complete detachment means a state in which the nanoparticles are uniformly distributed, not present in the agglomerated state in the polymer resin. In a sense, in particular, the ultrasonic homogenization is easy to separate aggregates to the homogeneous phase.

When ultrasound propagates through a resin with encapsulated nanoparticles, bubbles created by cavitation are generated in the colloid solution. Due to pressure difference between ultrasound and the solution, the bubbles burst, which locally generate a jet flow forming a pressure gradient. Due to this phenomenon, the nanoparticles that are bound to each other through van der Waals force are separated, and form a homogeneous dispersion within the resin matrix. (Manson & Sperling, 1976 cited in Park & Lee, 2011).

That is, the nanoparticles are dispersed by ultrasonic homogenization. The ultrasonic wave is applied not only to nanoparticles but also to the polymer matrix. The ultrasonic waves as mechanical vibration propagate through very close displacements of atoms and chain segments from their equilibrium position. So in polymers, the forces acting along the chain segments and between chains of molecules enable displacements into adjoining places, thus, generating stress waves through the material (Krautkramer & Krautkramer, 1977 cited in Lionetto & Maffezzoli, 2013).

The ultrasonic homogenization process depends on a variety of parameters, such as amplitude, pressure, temperature, viscosity and concentration. All of them, the important parameter configuration indicates a function of the energy per processed volume. The function alters with a change in the individual parameters. Also, the actual power output per surface area of the sonotrode of an ultrasonic unit relies on

the parameters (Hielscher, T., 2005). A sonotrode is a tool, which creates ultrasonic vibrations and applies this vibrational energy to a gas, liquid, solid or tissue in ultrasonic machining.

In general, the greater the intensity of the ultrasonic dispersion in the output power the greater the effect of the nanoparticles themselves and the effects are different depending on the type of nanoparticles. It is not true that a high output power can produce a uniform dispersion. The results of the impact and tensile test showed that nanocomposites dispersed at 45W of ultrasonic intensity displayed a specific trend, while the dispersion condition of 60W showed none.

And to conclude, 0.5 wt.% 700HTHNTs nanocomposite showed the best reinforcing effect and for amounts over 0.5 wt.% the reinforcing effect decreased markedly. The 700HTHNT acted as a defective element not as a reinforcement material. By contrast, 1000HTHNT nanocomposite showed a reinforcing effect and showed a great amount of strength when the content was 1 wt.%. The reinforcing effect became high when the content was more than 1 wt.%. Therefore, for the ultrasonic dispersion at 45W, the nanocomposites with 0.5 wt.% 700HTHNTs and 1 wt.% 1000HTHNTs were considered as optimum conditions.

For ultrasonic dispersion condition of 60W, there was no tendency of normalizing possibility in the results of the tensile and impact test. The 1000HTHNT showed excellent tensile strength for the ultrasonic dispersion of 45W also was recorded for the low impact strength. The ultrasonic dispersion intensity of 60W was believed as a not suitable condition for dispersion of the heat-treated HNT.

Chapter 4 Conclusion

In this study, the UP and HNT based nanocomposites were developed. The HNTs were divided into 5 types; untreated HNT (UTHNT), 300°C heat treated HNT (300HTHNT), 500°C heat-treated HNT (500HTHNT), 700°C heat-treated HNT (700HTHNT) and 1000°C heat-treated HNT (1000HTHNT). Two values of the output power of ultrasonic homogenizer were used, viz. 45W and 60W the HNT dispersion in UP. The mechanical properties were investigated through impact and tensile test. The reinforcement effects of HNTs that were heat treated at various temperatures and the dispersion behavior of nanoparticles in the matrix with various amount of HNTs (0.5, 1 and 3 wt.%) were also investigated.

The current study aimed to find the optimal dispersion condition in order to produce the UP/HNT nanocomposites with excellent mechanical properties. Experimentally, the results obtained are as follows:

(1) When the temperature of heat treatment was increased, structural changes of HNT were observed. The partial unification of layer structure began through dehydration from 500°C and almost every layered structures observed were destroyed at about 1000°C. Also, the rough surfaces and inhomogeneous areas increased with temperature. The decomposition of the HNT structure and generation of metakaoline phases occurred at 700°C and the HNT adopted an amorphous structure at 1000°C. Since HNT is sensitive to heat so the structure changed on heating.

(2) The reinforcement effect of HNT was partially realized. Results of impact and tensile test showed that impact reinforcing effect was higher than the tensile reinforcement effect under same conditions. In terms of impact reinforcing effects, the 700HTHNT nanocomposite was superior with high impact strength. At 45W of output power, the 0.5 wt.% HNTs in UP showed good reinforcement properties. Also, the reinforcement properties of 1 wt.% HNTs was cut out for condition of 60W output power.

(3) Especially in tension, there were almost no reinforcing effects of HNT. It is considered that the changes in the process and material controlling method is needed and the dispersion method and conditions, such as in this study, is meaningless.

(4) The rheological property of matrix resin was affected by HNT. The more HNTs added, the more the aggregation of HNT as clusters occurred. However, the nanocomposites reinforced HNT were also limited according to the types of untreated or heat-treated HNT, the dispersion method, manufacturing process conditions of samples and performance evaluation method of samples.

Reference

- Albdiry, M.T. Ku, H. & Yousif, B.F., 2013. Impact fracture behavior of silane-treated halloysite nanotubes-reinforced unsaturated polyester. *Engineering Failure Analysis*, 35, pp.718-725.
- Albdiry, M.T. & Yousif, B.F., 2014. Role of silanized halloysite nanotubes on structural, mechanical properties and fracture toughness of thermoset nanocomposites. *Materials and Design*, 57, pp.279-288.
- Abdullayev, E. & Lvov, Y., 2010. Clay nanotubes for corrosion inhibitor encapsulation: release control with end stoppers. *The Royal Society of Chemistry*, 20, pp.6681-6687.
- An, J.P. & Park, J.G., 2006. Diffraction principles of electron microscopy and applications of nanostructures analysis. *The Polymer Society of Korea*, 17(4), pp.493-501.
- Carli, L.N. Daitx, T.S. Soares, G.V. Crespo, J.S. & Mauler, R.S., 2014. The effects of silane coupling agents on the properties of PHBV/halloysite nanocomposites. *Applied Clay Science*, 87, pp.311-319.
- Chiu, H.T. Jeng, R.E. & Chung, J.S., 2004. Thermal cure behavior of unsaturated polyester/phenol blends. *Journal of Applied Polymer Science*, 91, pp.1041-1058.
- Deen, I. & Zhitomirsky, I., 2014. Electrophoretic deposition of composite halloysite nanotube-hydroxyapatite-hyaluronic acid films. *Journal of Alloys and Compounds*, 586, pp.S531-S534.
- Deng, S. Zhang, J. & Ye, L., 2009. Effects of chemical treatment and mixing methods on fracture behavior of halloysite-epoxy

nanocomposites. The International Committee on Composite Materials (ICCM).

Deng, S. Zhang, J. & Ye, L., 2009. Halloysite-epoxy nanocomposites with improved particle dispersion through ball mill homogenization and chemical treatments. *Composites Science and Technology*, 69, pp.2497-2505.

Frost, R.L. & Kristof, J., 1997. Intercalation of halloysite: a raman spectroscopic study. *Clays and Clay Minerals*, 45(4), pp.551-563.

Frost, R.L. & Shurvell, H.F., 1997. Raman microprobe spectroscopy of halloysite. *Clays and Clay Minerals*, 45(1), pp.68-72.

Fujii, K. Nakagaito, A.N. Takagi, H. & Yonekura, D., 2013. Sulfuric acid treatment of halloysite nanoclay to improve the mechanical properties of PVA/halloysite transparent composite films. *Composite Interfaces*, 21(4), pp.319-327.

Hielscher, T., 2005. Ultrasonic production of nano-size dispersions and emulsions. Dans *European Nano Systems Workshop-ENS*.

Jia, Z.X. Luo, Y.F. Yang, S.Y. Guo, B.C. Du, M.L. & Jia, D.M., 2009. Morphology, interfacial interaction and properties of styren-butadiene rubber/modified halloysite nanotube nanocomposites. *Chinese Journal of Polymer Science*, 27(6), pp.857-864.

Joo, Y.H. Sim, J.H. Jeon, Y.J. Lee, S.U. & Sohn, D.W., 2013. Opening and blocking the inner-pores of halloysite. *Journal of the Royal Society of Chemistry*, 49, pp.4519-4521.

Kamble, R. Ghag, M. Gaikawad, S. & Panda, B.K., 2012. Halloysite nanotubes and applications: a review. *Journal of Advanced Scientific Research*, 3(2), pp.25-29.

- Kim, D.H. Zheng, X.R. Kim, M.S. & Park, C.W., 2015. Influences to additive type on carbon nanotube metal composite. *Journal of the Korean Society for Composite Materials*, 25(5), pp.159-163.
- Kim, Y.H. Park, S.J. Lee, J.W. & Moon, K.M., 2015. A study on the effect of halloysite nanoparticle addition on the strength of glass fiber reinforced plastic. *Modern Physics Letters B*, 29, pp.154003.
- Na, H.Y. Yeom, H.Y. Yoon, B.C. & Lee, S.J., 2014. Cure behavior and chemorheology of low temperature cure epoxy matrix resin. *Polymer (Korea)*, 38(2), pp.171-179.
- Lee, J.M. & Cho, D.W., 2003. Cure behavior, thermal stability and flexural properties of unsaturated polyester/vinyl ester blends. *Polymer (Korea)*, 27(2), pp.120-128.
- Lionetto, F. & Maffezzoli, A., 2013. Monitoring the cure state of thermosetting resins by ultrasound. *Materials*, 6(9), pp.3783-3804.
- Li, X. Nikiforow, I. Pohl, K. Adams, J. & Johannsmann, D., 2013. Polyurethane coatings reinforced by halloysite nanotubes. *ACS Applied Materials & Interfaces*, 3, pp.16-25.
- Osman, E.A. Vakhguelt, A. Sbarski, I. & Mutasher, S.A., 2012. Curing behavior and tensile properties of unsaturated polyester containing various styrene concentrations. *Malaysian Polymer Journal*, 7(2), pp.46-55.
- Pal, P. Kundu, M.K. Kalra, S. & Das, C.K., 2012. Mechanical and crystalline behavior of polymeric nanocomposites in presence of natural clay. *Open Journal of Applied Sciences*, 2, pp.277-282.
- Park, J.H. & Kim, J.Y., 2002. The role of nano-particles on the material

- properties of epoxy/ nano-composites. *Journal of the Korean Society for Aeronautical & Space Science*, 30(5), pp.88-93.
- Park, J.J. & Lee, J.Y., 2011. Dispersion technology of layered silicate nanoparticles. *Bulletin of the Korean Institute of Electrical and Electronic Material Engineers*, 24(11), pp.3-14.
- Prashantha, K. Lacrampe, M.F. & Krawczak, P., 2013. Halloysite nanotubes-polymer nano composites: a new class of multifaceted materials. *Advanced Materials Manufacturing & Characterization*, 3(1), pp.11-14.
- Romanzini, D. Frache, A. Sandro, A.J. & Amico, S.C., 2015. Effect of clay silylation on curing and mechanical and thermal properties of unsaturated polyester/montmorillonite nanocomposites. *Journal of Physical and Chemistry of Solids*, 87, pp.9-15.
- Smith, M.E. Neal, G. Trigg, M.B. & Drennan, J., 1993. Structural characterization of the thermal transformation of halloysite by solid-state NMR. *Applied Magnetic Resonance*, 4, pp.157-170.
- Wang, Q. Zhang, J. Zheng, Y. & Wang, A., 2014. Adsorption and release of ofloxacin from acid-and heat-treated halloysite. *Colloids and Surfaces B: Biointerfaces*, 113, pp.51-58.
- Yuan, P. Tan, D. Faiza, A.B. Yan, W. Fan, W. Fan, M. Liu, D. & He, H., 2012. Changes in structure, morphology, porosity, and surface activity of mesoporous halloysite nanotubes under heating. *Clays and Clay Minerals*, 60(6), pp.561-573.
- Zhang, Y. He, Xi. Ouyang, J. & Yang, H., 2013. Palladium nanoparticles deposited on silanized halloysite nanotubes: synthesis, characterization

and enhanced catalytic property. Scientific Reports, 3(2948).



감사의 글

이 ‘감사의 글’을 적을 날이 올지 몰랐습니다. 막상 제 이름 석 자가 박힌 논문에 마침표를 찍으려하니 어떤 말로 운을 떼야할지 막막하기만 합니다.

학위 과정을 밟던 지난날과 그 순간을 함께 했던 사람들. 단지 이 논문은 연구라는 한 부분의 결과일 뿐이지만 연구를 목적으로 선택했던 복합 재료 실험실에서의 4년이란 시간은 한 마디로 표현하지 못할 만큼 많은 가르침과 경험을 주었습니다. 함께하는 기쁨을 알게 해 주었고 힘듦을 같이 극복할 수 있다는 믿음을 갖게 해주었습니다. 생각은 단지 머릿속에만 머무는 것이 아니라 표현할 수 있는 것임을, 그리고 그 것에는 경계가 없다는 것을 배웠습니다.

석사 과정을 밟으면서 정말 많은 사람을 만났습니다. 다양한 이야기를 나눴고 서로의 생각을 공유했습니다. 특히, 일본에서 수학했던 1년은 앞으로 살아갈 날과 함께 제 인생에서 가장 중요한 전환점이 되었습니다. 저의 외면뿐만 아니라 내면까지도 바꿔놓았으며, 다가올 날에 대한 기대를 심어주었고 여전히 불분명한 미래지만 ‘꿈’에 대한 막연함과 막막함보다는 현실로 만들 수 있다는 용기와 희망을 보여준 시간이었습니다. 다양한 나라의 사람들을 만났습니다. 일본, 중국, 대만, 독일, 인도, 브라질 등, 우리의 공통분모는 연구를 하는 사람 혹은 연구를 하는 사람이 되고 싶은 사람이었지만 각각의 만남 뒤엔 연구에 대한 성과보다는 사람과 사람의 관계, 그리고 그들의 생각을 통한 깨달음이었습니다.

그래서 저는 말할 수 있습니다. 감사합니다, 김윤해 교수님. 이 말엔 그 어떤 수식어도 필요치 않습니다. 다만 많은 기회를 주었고 그 기회를 잡을 수 있게 용기를 준, 그리고 언제나 웃으며 곱씹을 수 있는 소중한 추억과 만남을 나눠준 교수님께 감사의 인사 전합니다.

고맙습니다. 저와 좋은 관계를 맺어 준 선배·후배님- 하진철 선배님, 시작을 함께 해주시고 좋은 말씀으로 여기까지 잘 이끌어주셔서 감사합니다. 박세호 오빠, 생각만 하는 것보다 일단 결단을 내리는 것, 그리고 그것을 온 힘 다해 해보는 것이 중요하다는 것을 많이 느꼈습니다. 해보지 않았으면 절대 몰랐을 것들에 대해 정말 감사드립니다. 윤성원 오빠, 첫 만남부터 많이 의지를 했었던, 그래서 더 부담스러웠을 것 같은 생각이 들지만 그렇게 4년이라는 시간동안 연을 맺어 왔습니다. 어떤 말로도 그 많은 배움 값을 순 없겠지만 더 좋은 모습 드릴 수 있도록 하겠습니다, 항상 고맙습니다. 이진우 오빠, 떠올리면 마냥 웃을 수만은 없을 것 같은 날들이 이제는 웃으며 이야기를 할 날이 왔습니다. 뒤돌아보면 그 시간들이 있어 그 때 보다 지금의 제가 더 단단해졌음을 느낍니다. 많이 배웠습니다. 감사합니다. 정민교 오빠, 늘 부족하고 느린 후배였지만 차근차근 잘 이끌어줘서 고맙습니다. 매 중요한 순간마다 늘 힘이 됐던 오빠가 있어 감사합니다. 박창욱 오빠, 우선, 일본에서 받았던 식료품 상자는 절대 잊지 못할 겁니다. 조금 늦게 알게 된 인연이지만 앞으로 알아갈 날이 더 많을 테니 다행이라고 생각합니다. 표현이 서툰 후배라 늘 툭툭대기만 하는데 이렇게나마 전합니다. 감사합니다.

유정오 오빠, 정경석, 원치형, 김세운, 김한솔, 심영훈, 김경원, 김별 모두에게- 살갑기보다는 오히려 무덤덤한 저와 함께해줘서 감사하단 말 전하고 싶습니다. 그리고 신동일 오빠, 비록 같은 연구실은 아니었지만 알고 지냈던 모든 순간들에 웃을 수 있었고 많은 정신적 가르침에 감사합니다. 그리고 이 외 모든 만남을 함께 해준 분들께 감사합니다.

감사합니다, Hanabusa Takao 교수님, Antoni Norio Nakagaito 교수님, Hitoshi Takagi 교수님. 서툰 일본어와 영어를 이해해주시고 믿음으로 이끌어주셔서 일본에서의 생활이 따뜻했었습니다. 어떠한 관계를 맺기에 턱없이 부족했던 시간이었지만 떠올리면 미소를 지을 수 있어 더 소중한 시간이었습니다. Hisyam, Rosni, Sakaki, Ueno, Nishimura, Marco Wittlich, Shoui, Iemura 모두들 낯선 이방인을 따뜻하게 받아줘서 고맙습니다. 특

히, Sun Wan Ting, 우린 같은 처지였고 그래서인지 더 많이 의지했던 것 같습니다. 이젠 각자의 자리에서 또 다른 내일을 그려가겠지만 옆에 없어도 항상 응원하고 행운을 빌어주겠습니다. 더 좋은 모습으로 다시 만날 날을 기대할 수 있는 친구여서 참 고맙습니다.

감사합니다, 김수현 언니, 배지영 언니. 언니들이 없는 일본 생활은 정말 반쪽일 것 같습니다. 어떤 말보다도 하고 싶은 말은 우리 오래오래 더 많은 추억 만들어봅시다. 언니들이 있어 행복하고 따뜻했던 시간이었습니다, 이 논문을 잘 마칠 수 있게 든든하게 있어줘서 정말 고맙습니다.

끝으로, 가족에게 단 한 번도 제대로 하지 못했던 이 말 적습니다. 대학에 들어오면서부터 바깥 생활하느라 이런저런 핑계에 늘 집보단 밖으로 걸돌던 둘째지만, 그래도 믿어주고 이해해주고 그 어떠한 순간에도 내 편이 되어주셔서 감사합니다. 앞으로도 웃을 날, 울 날 많겠지만 그럴수록 더 함께이길 바랍니다. 사랑합니다.



- 2016년 1월 28일

2년 동안의 결실을 맺으며.